

Article

The Dynamics of Transformation of Lithospheric Mantle Rocks Beneath the Siberian Craton

Yury Perepechko ¹, Victor Sharapov ^{1,*}, Anatoly Tomilenko ¹, Konstantin Chudnenko ², Konstantin Sorokin ¹ and Igor Ashchepkov ^{1,*}

¹ Sobolev Institute of Geology and Mineralogy, Siberian Branch of the Russian Academy of Sciences, 630090 Novosibirsk, Russia; yuri@perep.ru (Y.P.)

² Vernadsky Institute of Geochemistry, Siberian Branch of the Russian Academy of Sciences, 664033 Irkutsk, Russia

* Correspondence: vik@igm.nsc.ru (V.S.); igor.ashchepkov@igm.nsc.ru (I.A.)

Abstract: The problem of heat–mass transfer in the permeable areas above the asthenosphere zones was numerically studied based on an examination of the inclusion content in the minerals (olivine and clinopyroxenes) of igneous and metamorphic rocks of the lithospheric mantle and the Earth’s crust; evaluations of thermodynamic conditions of the inclusion formation; and experimental modeling of the influence of hot reduced gases on rocks in the mantle beneath the Siberian craton. The flow of fluids of a certain composition from the upper-mantle magma chambers leads to the formation of zonal metasomatic columns in the ultrabasic mantle lithosphere in the permeable zones of deep faults (starting from the lithosphere base at 6–7 GPa). When petrogenic components enter from the magma pocket, depleted ultrabasic lithospheric mantle rocks change to substrates, which can be considered as the deep counterparts of crustal rodingites. Other fluid compositions result in strong calcination and pronounced salinization of the metasomatized substrates or an increase in the garnet content of the primary ultrabasic matrix. A region of alkaline rocks forms above these areas, which changes to pyroxenes, amphiboles, and biotites. The heat–mass transfer modeling for the two-velocity hydrodynamic model shows that gas–fluid and melt percolation lead to an increase in the thermal front velocity under convective heating and a pressure drop in flow. It is also shown that grosspidites are considered to be eclogites, are found in the permeable zones of the lithospheric mantle columns serving as conduits for the melt/fluids and represent the products of the carbonated metasomatic columns. The carbonization caused by proto-kimberlite melts may essentially decrease the diamond grade of kimberlites due to carbon oxidation.

Keywords: Siberian craton; petrology; morphotectonics; heat–mass transfer; mathematical modeling



Citation: Perepechko, Y.; Sharapov, V.; Tomilenko, A.; Chudnenko, K.; Sorokin, K.; Ashchepkov, I. The Dynamics of Transformation of Lithospheric Mantle Rocks Beneath the Siberian Craton. *Minerals* **2023**, *13*, 423. <https://doi.org/10.3390/min13030423>

Academic Editor: Alexandre V. Andronikov

Received: 23 January 2023

Revised: 1 March 2023

Accepted: 10 March 2023

Published: 16 March 2023



Copyright: © 2023 by the authors. Licensee MDPI, Basel, Switzerland. This article is an open access article distributed under the terms and conditions of the Creative Commons Attribution (CC BY) license (<https://creativecommons.org/licenses/by/4.0/>).

1. Introduction

The dynamics of transformation of lithospheric mantle rocks under the Siberian craton (SC) has two aspects: (1) a change in mineral compositions of lithospheric rocks under the influence of conductive heat flow from the upper mantle, and (2) a change in the rock compositions of the lithosphere in the permeable zones (faults) during convective heating by mantle fluid flow, followed by metasomatic transformation of the primary rock matrix by melted/fluid-transported components. The first aspect is regarded as an inverse petrogenetic problem (estimations of temperature (T) and pressure (P) based on mineral equilibrium analyses), where mineralogical ‘thermometers’ and ‘barometers’ that are determined by the estimates of temperature and pressure for mineral association formation are correlated with ‘geotherms’ with corresponding heat flows [1,2]. If the mineral equilibria are influenced by local filtering of pore fluids, the inverse petrogenetic problem can be solved using a two-reservoir flow-type reactor with a stationary PT profile [3].

This work deals with the second aspect of the problem of metasomatic transformations of lithospheric mantle rocks. Both qualitative and quantitative models were used to analyze

the metasomatic processes petrogenetically [4,5]. A quantitative model for the dynamics of non-isothermal metasomatism under the lithospheric mantle was probably first formulated by F. Spera [6], where the process of convective heating and transformation of lithospheric mantle rocks by CO₂ flow (separated from the basic melt out of the magma source) was considered. The hydrodynamic parameters of the process were taken in this work as Darcy approximation.

The most difficult problem associated with the dynamics of convective mass–heat exchange is the setting of correct initial and boundary conditions for the endogenous processes. These data can be mainly obtained from a study of mantle-derived rock xenoliths in kimberlites and basic melts. The main information on fluids (penetrating from the asthenosphere’s magma chambers and responsible for convective transfer) is obtained from a study of their inclusions in minerals of mantle xenoliths and diamonds, as well as their inclusions in the minerals of igneous rocks that are the exported fragments of mantle rocks. In this work, this problem was investigated based on the methods for studying gas in mantle rocks, statistical processing of experimental data, and finding solutions for the direct problems of the dynamics of non-isothermal metasomatism [7–9]. A model [6] was developed based on the modification of the software Selector-C [10] as a flow-type multi-reservoir reactor [8,9]. Further development of the model means the construction of a more realistic multi-phase hydrodynamic model.

The results of our modelling may be found in the Supplementary File S1, (SP1), Tables S1–S9.

2. Initial Information on the Compositions of Mantle Fluids in Metasomatic Rocks from the Lithospheric Mantle Beneath the Siberian Craton

Since we consider the dynamics of metasomatic alteration of mantle rocks, we need data on the real compositions of fluids preserved in lithospheric rocks. These data were obtained for metamorphic rocks from the earth’s crust and the lithospheric mantle.

2.1. Study of Composition and Thermobarometric Properties of Mantle Samples from the Lithospheric Mantle under the Siberian Craton

Asthenosphere fluids derived from various plume melts (kimberlitic, basaltic carbonatitic, and ancient subduction-related melts) influence the lithospheric mantle, probably through the interaction with melts and relatively reduced fluids [5]. We can expect a great variety of volatile compounds for the C-H-O-N-S system if these fluids are generated by basic melts that appear during the decompression melting of upper mantle rocks [10,11]. Therefore, their products of interaction with lithospheric rocks vary. These variations have been discussed in many published papers [12–25]. The results of these studies can be generalized in the following way: (1) an increase in C/H modulus causes a decrease in H₂O and CH₄ contents; (2) an increase in O content causes an increase in the oxidation of gas mixture; (3) the presence of C in solid phase stabilizes the ration of gases in the mixture; (4) the composition of heavy hydrocarbons (HHC) and light hydrocarbons (LHC) changes in a certain way when PT conditions change; and (5) during the non-stationary stage of fluid–rock interaction, rock buffers (the content of metals of varying valence) are responsible for the change in the gas mixture’s compositions.

Mineral and fluid inclusion compositions for various metamorphic facies is another source of information about the products of heterophase interactions in the lithosphere [19,26–28]. We used the above-mentioned work in two subsequent stages: (1) obtaining sufficient statistical data on fluid composition in rocks of the lithosphere, from its base to the metamorphic layers of the earth’s crust, and (2) reviewing various studies on the physicochemical dynamics of fluid–rock interaction. Since xenoliths of lithospheric rocks are the main sources of study, there is a problem of uncertainty because of the hydro-mechanical separation of fragments in upcoming magma flows of mantle sources [29]. Therefore, there should be a representative observation set to help solve this problem. A. A. Tomilenko [7] presented a set of more than 110 crushed monomineral samples of mantle xenoliths of the main rock types from three pipes from the SC. For

metamorphic crust rocks, the set is larger—more than 300 probes. Some of the examples of the gaseous phase compositions of the mantle xenoliths and methods of gas analyses are represented in the SP1, Table S10. It also includes a general description of the methodology of the analytical methods.

Considering the results of the statistical processing of the obtained data, the most complete data set exists for the xenoliths from the Udachnaya diamond pipe (Supplementary File S1 (SP1), Table S1). The presence of gases, such as H₂O, CO₂, CO, H₂, and CH₄, was determined using the N. Osorgin's method [30] from the rock groups with the following numbers of samples: eclogites—11; spinel lherzolites—10; spinel–garnet lherzolites—14; dunites—21; and sheared lherzolites—21. The gas contents were as follows: in olivines (Ol)—73%; in garnets (Ga)—24%; and in clinopyroxenites (Cpx)—3%. The rock sequence in the first approximation coincides with the model profile of the thickest craton lithosphere [31]. It was found (Table S1) that both the contents and gas ratios of all rock groups can be divided into three or four clusters (water-enriched (H₂O/Σ(CO₂+CO+CH₄+H₂)) and water-reduced (CO₂/Σ(CO+CH₄+H₂)): there are both high-water content and low-water content clusters, with relatively low-water clusters containing more reduced gases (reduction modulus is up to twice as less as in high-water content samples).

2.2. Comparison of Fluid Compositions in Diamonds and Minerals of Kimberlites and Xenoliths of Mantle Rocks

The analysis of the obtained data shows that sheared garnet lherzolites are resulted from the latest processes of water enrichment and refertilization correspondent to the protokimberlite metasomatism. According to [31], these rocks underlie the other studied rock groups in the craton lithosphere; thus, these xenolith samples are taken as the objects for the numerical modelling of physicochemical interaction between over-asthenosphere fluids and lithospheric rocks. Therefore, the fluid parameters for this rock group and olivines from kimberlites (SP1, Table S1, Figure 1), as well as fluid inclusions in diamonds, are most interesting to obtain a solution for the problems of equilibrium physicochemical dynamics of interaction between over-asthenosphere fluids and lithospheric rocks under the SCs. The clusters of sheared lherzolites represent the following amounts of the whole sample analysis: cluster #1—14.3%; cluster #2—28.5%; cluster #3—47.6%; and cluster #4—9.5%. Therefore, we can take the composition of cluster #3 as the characteristic bulk composition for over-asthenosphere fluids in the deepest lithospheric rocks under this SC.

Using a step-by-step thermal decrepitation of one of the samples of this cluster, we found the following sequence for gas separation: At up to T = 600 °C, about 72% of CO₂, 59% of H₂O, and 36% of CH₄ are separated. When T > 800 °C, 100% of H₂, 100% of CO, 49% of CH₄, 34% of H₂O, and 28% of CO₂ are separated. This procedure has been described in [30,32]. Thus, the high-temperature gas mixture has the following composition: H₂O—54%; CO₂—9%; CO—27%; H₂—9%; and CH₄—1%. It should be noted that a similar sequence of thermal fluid separation was observed in the samples of garnet lherzolites and eclogites.

Taking into account that the minerals of the studied rocks include primary (referring to ancient magmatic stages) and secondary (after the reactions) gas and gas–liquid inclusions, we can suggest that there is a rather wide temperature interval for fluids' influence on inclusion rocks. The local intensity of these processes for both the same facies and facies at various depth substantially differs. There are at least two temperature stages for the interaction of mantle and crust fluids with the rocks presented in xenoliths: (1) the mantle stage of T~900 °C and higher, and (2) the crust stage (during the development of diatreme and the interaction between magma body and pore fluids of the host crust rocks), with T < 800 °C. The method of gas phase determination in inclusions [7] is based on mineral probe sampling with thorough processing of crystal surfaces from the secondary changes. The statistical data given above show only heterophase interactions for the mantle stage of rock change.

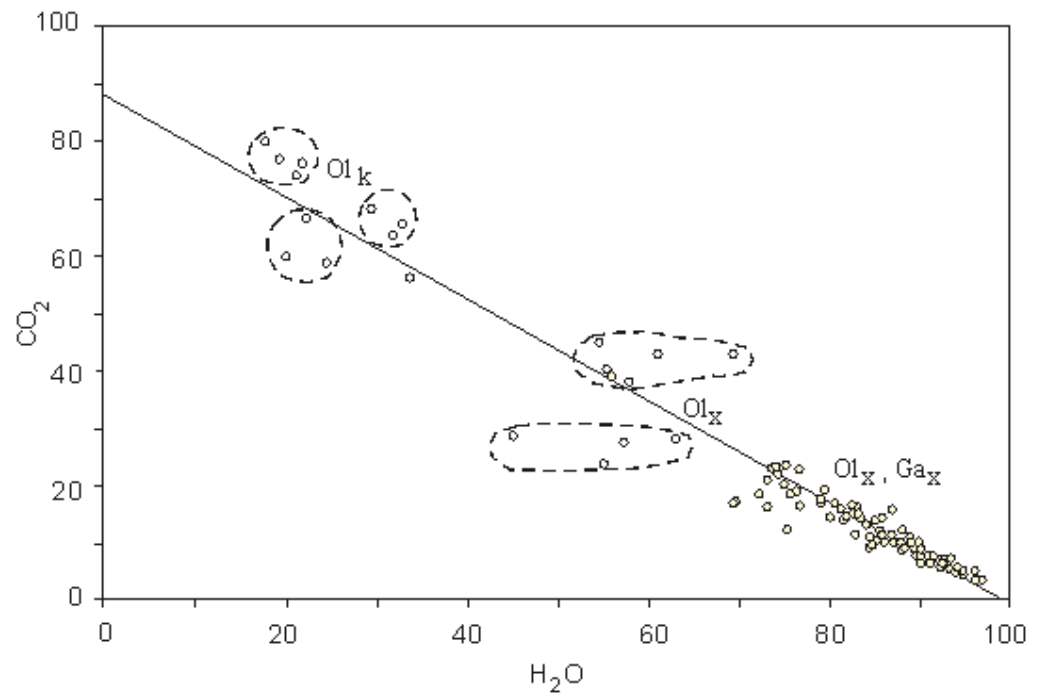


Figure 1. Proportions of the bulk CO₂ and H₂O contents in olivines (Ol_x) and garnets (Ga_x) from the xenoliths of mantle ultrabasic rocks and ‘eclogites’ (Udachnaya–Vostochnaya, Mir, Obnazhenaya (Yakutia), and Victor Roberts (South Africa) diamond pipes). Ol_k—magmatic olivines from kimberlites of the Udachnaya–Vostochnaya pipe.

These data are complemented by the results of gas studies examining eclogite xenoliths from the kimberlite pipes: Mir (Ga, the number of samples $n = 7$); Obnazhenaya (Ga, $n = 15$)—(our data from SC); and Roberts Victor (South Africa) (collected by N. V. Sobolev) (Ga, $n = 3$). The data for the above-mentioned gases do not differ greatly from the results for garnets in eclogites for the Udachnaya Pipe. Therefore, the data presented in Table S1 can be regarded as typical for the fault zones of SP lithosphere for all the diamond-bearing areas. The whole distribution for CO, CO₂, and H₂O ratios with the same data of olivine phenocrysts in kimberlites for the Udachnaya–Vostochnaya pipe is shown in Figure 1. The trends in this data set are determined by the following formulas: CO₂ = 88 – 0.89·H₂O (%), and CO = 10 – 0.09·H₂O (%). This trend includes 80% of observations, with water contents between 72%–94%. Some value groups are formed within this trend, representing 5%–10% swarms of total observations. The ratios CO↔H₂O and CO↔CO₂ do not show distinct dependences: for CO↔CO₂, the correlation coefficient is $r = +0.3$; for CO₂↔H₂O, $r = -0.91$; and for CO↔H₂O, $r = -0.6$. Thus, no less than 80% of fluid mixtures in mantle xenoliths refer to a sequence of fluids with high-water content, where the increase in water content causes a linear decrease in both CO₂, and CO.

The statistical data on gas compositions in inclusions in diamonds show similar principles [28,33–35]. Our explorations [33–38] have concentrated mainly on mantle minerals and rocks (SP1, Table S1). The average content for gas mixture components in the ‘analyzed diamonds is as follows: H₂O—85.3%, CO₂—10.1%, CH₄—1.15%, N₂—3.1%, C₂H₆—0.02%, C₃H₈—0.05%, C₄H₁₀—0.115%, and C₅H₁₂—0.11%. Within these samples, we can distinguish six clusters; the cluster for $n = 6$ has the following mean values: H₂O—89.75%, CO₂—8.21%, CH₄—0.53%, N₂—8.73%, C₂H₆—0.02%, C₃H₈—0.0%, C₄H₁₀—0.734%, and C₅H₁₂—0.0%. The linear correlations within the whole samples set are different from those of gas fluids from the main mineral matrixes of mantle rocks: for H₂O↔CO₂, $r = -0.87$; for H₂O↔N₂, $r = +0.53$; and for CH₄↔C₃H₈, $r = +0.65$. The linear trend is determined by the formula CO₂ = 70.84 – 0.71·H₂O (%) (where r is the reliability of the correlation coefficient).

The comparison of gas compositions in diamonds and olivines from the xenoliths of ultrabasic rocks have the following peculiar features: high water contents and rather low CO₂ concentrations, and an absence of substantial CO and H₂ contents with rather high amounts of CH₄ and N₂. The most interesting physicochemical characteristics of the gas mixture composition for the fluid inclusions of diamonds is the absence of light hydrocarbons, such as C₂H₂, and a high concentration of heavy hydrocarbons, such as C₃H₈, C₄H₁₀, and C₅H₁₂. The fluids in diamonds are more reduced than the fluids in xenoliths, and CO and H₂ are practically absent.

The statistical analysis of gas compositions in the rock inclusions of granulite and amphibolite facies shows a rather different (from the lithospheric mantle) fluid phase composition [7,36,37]. According to the results of the study on individual inclusions using CS spectroscopy, carbonic acid fluids with a low water content probably dominate in the granulite complexes of the SC. Of all the studied rocks (n = 302), about 76% are carbon acid fluids, and rocks with a high nitrogen rocks are about 19%, with the following average contents: N₂—95%, CO₂—3.9%, and CH₄—1.22%. A very small part of the studied samples is presented by nitrogen–methane (2.3%) and methane–carbon acid (2.6%) fluids. It is interesting to note that such compositions are typical for both garnet-containing rocks and rocks of amphibolite facies. All studied metamorphic rock masses of the above-mentioned anomalous fluid compositions belong to folded structures with overthrusts, boudinage of basic igneous rocks, and local super-high-pressure manifestations (Kokchetav Block, etc.). All fluids of the crust metamorphogenic rocks of the facies under consideration have negative correlation ratios for the above-mentioned macro-gases: for CO₂↔CH₄, r = −0.32, and for CO₂↔N₂, r = −0.95. These relations are typical if we take into account the volume of sampling.

2.3. Petrogenetic Features of Total Gas Compositions in Minerals of Xenoliths

Our obtained statistical results allow us to formulate some conclusions on the general and local characteristics of metamorphogenic deep-seated fluid systems. They include data for the samples from mantle lithosphere of the craton and crust rocks under the Conrad discontinuity.

The total principles of equilibrium hydrocarbon content changes for various facies of SC mantle rocks are given by [24,25]. They show that the main peculiarity of hydrocarbon (HC) composition change (because of temperature and pressure changes in the upper mantle) is the presence of the ‘methane threshold’: the transformation of heavy HC into light HC that, according to the numerical experiments, are close to ‘diamond-graphite’ equilibrium parameters [38]. These principles can be distorted by catalytic processes [38–41], which are not studied experimentally for the lithospheric mantle P-T parameters. Oxygen-containing HC behavior is a special problem because, according to the numerical experiments, for T > 1200 °C, they can compile more than 50% of total fluid-phase mass. These compounds cannot be determined using standardized chromatographic analysis. They were also not studied in our experiments the CEOCIT flow-reactor equipment [41].

The results of the theoretical analysis on mantle fluid compositions are sufficient to understand the trends of heterophase interactions, but they cannot help us solve the problem of bulk compositions of overbalanced gases and primary compositions of over-asthenosphere magma fluids. This statement can be illustrated by the following experimental data [36–40]: in these rocks’ primary molten inclusions and under the P-T conditions of metasomatism, the amphibole aggregates are altered into specific solid-phase structures (containing liquid carbon acid), which are associated with rocks with a complex of secondary mineralogical associations (coronary structures, amphibolization, quartz precipitation, plagioclase ‘deoxidation’, etc.). As the calculation for the equilibrium compositions of magmatogenic fluids in closed systems with basic rocks show (P-T conditions of amphibolite and spinel facies [42]), the composition of the gas phase (appearing after heterophase interaction) can vary substantially, depending on the initial H/C ratio in the gas phase. For example, the ratios of H₂O to CO₂ ratios depend on the initial H/C and pO₂ ratios for the gained P-T

conditions. For reduction systems when $H/C > 1$, $P < 10$ kbar, and $T < 750$ °C, nitrogen is prevailing in the gas phase, while under $T > 700$ – 750 °C, the gas phase is nitrogen–methane. The presence of graphite in the solid phase undoubtedly proves the existence of the above-mentioned conditions. However, the mono-carbon acid composition of the final gas phase for the considered equilibriums is not typical. It is possible that in primary molten inclusions, carbonic acid prevails, that is, during metamorphic over-balance in a closed system, the only gas composition of the solid phase and vacuole morphology is changed, while the bulk carbon acid composition of the gas phase is the same as a whole. This can be proven by the results of the study on the primary molten inclusions in the samples of gabbro-anorthosite crustal xenoliths from the Udachnaya kimberlite pipe [43]. In the clinopyroxene of these rocks, partly or completely crystallized melt inclusions with liquid carbon acid and syngenetic fluid inclusions of liquid carbon acid are found. The latter is also found in plagioclase and amphibole. On the other hand, as the results of the study of the gas phase in the phenocrysts of olivines in kimberlites of the Udachnaya pipe show, the gas compositions in melt inclusion contain both carbon acid and water [7,37].

The characteristics of gas phases in the inclusions of minerals from the sections of regional metamorphism of granulite and amphibolite facies and lithospheric mantle rocks in the zones of regional faults (controlling basic melts conduits) are substantially different. In the fault zone, during magma flow, under the pressure of about 8 kbar, an anorthosite magma body exists in the lithosphere; the gas phase of this magma body is practically represented by only carbon acid.

A comparison of these results on bulk gas composition in the minerals of xenoliths of lithospheric ultrabasic rocks from this magma flow (SP1, Table S1) shows their great difference. Moreover, for mantle rocks created in various depth, there is no general trend between the compositions of gases based on their average values, both for the individual clusters and complete sample (SP1, Table S1). However, the presence of general linear trends of ‘oxidation’ and ‘water-enrichment’ shows that there is a process of magma fluid over-balance, typical for all lithospheric mantle facies. On the other hand, the existence of three separate composition swarms (with various compositions of CO, CO₂, and H₂O) along with the linear trends (Figure 1) suggest that the compositions of magmatogenic gases (working during various stages of magmatogenic activity of the fault zones) are different. It should be noted that the data presented in SP1, Table S1 do not agree with the estimates for zonal T-P conditions for equilibrium gas mixture compositions of continental lithospheric mantle [24,25]. Thus, the fault zones are probably special lithospheric areas because of the composition of over-balanced magmatogenic fluids. All intraplate magma events within the SC are confined by deep faults [20,44,45]. Therefore, we suggest that to analyze the nature of clusters with fluid content in sheared lherzolites and other rocks in the lithospheric mantle under the craton of the Udachnaya pipe and to understand the reason for the bulk composition variation in the minerals of mantle rocks, it is important to study non-isothermal physicochemical dynamics of ‘fluid-rock’ interaction. It is necessary to solve the following problems: for the zone of kimberlite melt movement, we should find the magma gas fluid compositions, when these gas fluids dissolved in magmas influence the mantle rocks creating sheared lherzolites, and the bulk compositions the interacting rocks at the lithospheric mantle base. If it is not possible to find the compositions of magma gas mixtures, it is necessary to find processes of metamorphic over-balance for products of the preceding metasomatic process of mantle rock transformation that can result in fixed ratios for gas compositions in the most ‘water-enriched’ or ‘oxidized’ clusters from various metamorphic facies in the lithosphere.

3. Estimations of Compositions of Petrogenic Components Transported to Lithospheric Mantle Rocks by Metasomatic Fluids

To study inclusions in the minerals of ultrabasic rocks from the xenoliths of the Udachnaya–Vostochnaya pipe, we heated a polished plate of garnet lherzolite to $T = 1100$ °C in a thermal chamber. On the plate surface, at the olivine–orthopyroxene boundary,

we found drop-shaped accumulations of liquid phase with the following compositions: SiO_2 —79.7%, Al_2O_3 —2.5%, FeO —5.9%, MgO —2.1%, CaO —0.5%, Na_2O —1.5%, and K_2O —3.9% (by quenching, in glass). We also studied the primary and secondary inclusions in the minerals of the main rocks from the lithospheric mantle of this craton part [20]. The experiments were carried out using a heating equipment (Institute of Thermal Physics of SB RAN) containing a section of a flow reactor with the flow of reduced gases and a suitable temperature interval of 800–1200 °C [32]. Similar experiments were also carried out earlier for the temperature interval of 150–500 °C, using a flow-reactor equipment from CEOCIT company [41].

3.1. Physical Experiments

In the flow reactor fed by the flow of reduced gases (emerged during the ignition of carbon dust by a stream of burning propane), synthesis gas streamed along the reactor wall where the thermocouples were located, and rock cubes of $2 \times 2 \times 2 \text{ cm}^3$ were put on the porcelain covers of the thermocouples (Figure 1). The center of sample #1 was located at 160 mm distance from the burner edge, the center of sample #2 was located at 510 mm distance, and the center of sample #3 was located at 850 mm distance. The gas samplers were located parallel to the thermocouples, and the gas composition was determined by gas analyzer TEST-1. The temperatures of the gas flow sequence within the three platinum and platinum-rhodium thermocouples decreased from 1200 °C to 800 °C, at $P \sim 1$ atm. The composition of the gas mixture was represented by the following compounds: $\text{H}_2 \approx 8$ –13%, $\text{CO} \approx 9$ –11%, $\text{CO}_2 \approx 17$ –18%, and $\text{N}_2 \approx 58$ –66%.

Although the equipment was suitable for convective rock heating in our experiment, it was difficult to support the stationary regime for combustion and flame jet density, and, therefore, constant temperatures on the sample's surfaces. Temperature fluctuations within the gas stream were significant because of flow pulsing. In two cases, uncontrolled flow temperature increase at the reactor entry reached 1400 °C; this resulted in the practically complete melting of rock cubes at the thermocouple #1. The dynamics of gas flow influence on the rock samples included the following stages: (1) preliminary heating up to $T > 700$ °C (about 3 min); (2) reaching the necessary regime (about 5–6 min); and (3) the regime of maximum heating within the temperature range of 50–1100 °C, according to the samples: for sample #1—1100–1200 °C, for sample #2—1000–1100 °C, and for sample #3—800–900 °C (15–17 min). Then, the reducer was switched off, and the samples were taken out and cooled in the air. Gas sampling and analysis were carried out during all stages of the experiment. Bulk gas compositions were studied in the samples using N. Osorgin's method [30] at the Institute of Geology and Mineralogy of SB RAS. Kinetic curves for gas emission from the xenoliths were constructed within the temperature intervals of 200, 400, 600, 800, 900, 1000 °C, using chromatography. data on xenoliths of basic and ultrabasic rocks from kimberlites of the Udachnaya–Vostochnaya pipe (Yakutia) (SP1, Table S1) (composing craton lithosphere mantle profile from Moho to the base of diamond facies) was taken for the experiments [19,31].

3.2. Gas Compositions of Minerals and Reaction Veins of Xenoliths

Without a preliminary study of gas compositions in the minerals of xenoliths, the above-mentioned approach would be incomplete. If we do not know the composition of gas phase separating during rock heating, we can understand neither the specific compositional features of solid-phase quenching in the products of the minerals' partial melting at the heating surface nor the reaction phenomena at the boundaries of the minerals inside the samples. These data are presented above. It should be noted that for all the cases, positive relationship for $\text{CO}_2 \leftrightarrow \text{CO}$ was observed. To estimate the kinetic parameters of gas emission from the samples during heating in the reactor, step-by-step bulk compositions were measured with decrypting graph using the above-mentioned methods (SP1, Tables S2 and S3).

The cluster analysis of gas contents in the minerals (olivines, garnets, and clinopyroxenes) of major rock groups and the estimates of their correlative relationships show that the xenoliths from the same mineral facies contain variously changed rocks with substantially different kinetics of gas emission during thermal excitation. A comparison of the data from (SP1, Tables S2 and S3) shows that the bulk composition of gases in these rocks is practically identical to that in major minerals. This fact allows us to extend the observed phenomena (of convective mass exchange during sample heating by the flow of hot synthesis gas) to individual samples, where the gas ratios in the corresponding rock clusters were calculated. It is important for our experiments that, in the studied samples of ultrabasic rocks, 50%–100% of water was separated from the rocks when they were heated up to $T = 800\text{ }^{\circ}\text{C}$, which is before melting. Therefore, the melt bubbling rates in the surface films and fractures inside different samples do not vary substantially. The results of gas separation after the experiments are the same (SP1, Table S3). For our thermodynamic calculation to solve the problem of convective heating of rocks in the permeable zone we can simplify the system. Taking into account the statistical data for different gas contents, we can use a binary fluid, $\text{CO}_2 + \text{H}_2\text{O}$, with a $\text{CO}_2/\text{H}_2\text{O}$ ratio from 1/3 to 1/10 as the first approximation. For the physicochemical modelling, the information on glassy-phase composition (obtained when the temperature of the samples does not exceed $1000\text{ }^{\circ}\text{C}$ and when there is no melting of rock-forming minerals, but petrogenic components are extracted from the primary and secondary inclusions) is important (Table S4). These data show that in the fluid phase, there is a transfer of petrogenic components; the average qualitative ratios of these components, normalized by SiO_2 , are as follows: TiO_2 —0.002; Al_2O_3 —0.39; FeO —0.098; MgO —0.016; CaO —0.036; Na_2O —0.007; and K_2O —0.02. The obtained data indicate the prevalence of the wehrlitization trend in deeply depleted ultrabasic rocks. On the other hand, the prevalence of potassium over sodium and magnesium in the studied xenoliths series shows that there are local specific features of lithospheric mantle transformation within this part of diamond-bearing Siberian craton. There are ‘sodium’ and ‘potassium’ areas in the Cenozoic basalts of Mongolia [46]. In the tholeiites of Perm-Triassic SC traps [42], spatial compositional zoning together with the complex variations in local lava profiles were revealed. This shows that there are substantial variations in the compositions of rock matrix, which produce basic liquids (melts) under various cratons, and grabens in the Asian continental plate. Numerical modeling of the dynamics of metasomatic processes can explain physicochemical factors causing these phenomena.

4. Model of the Hydrodynamics of Metasomatic Transformation of the Lithosphere in the Permeable Zones under the Siberian Craton

In this work, we consider a process of heterophase non-isothermal interaction between fluid and rock based on the study of the thermo-mass exchange between the ideal gas mixture of fluid phase and solid phase was used for the approximation of a multi-reservoir flow reactor. The physicochemical dynamics of metasomatic change in lithospheric mantle rocks are based on the model of heterophase ‘fluid-rock interaction’ [47]. A kinetic model for heterophase reactions has not been constructed for petrogenetic problems [48], because neither the real thermodynamic constants for the phases of reaction during the heterophase interaction nor their kinetic characteristics, even for simplest reactions, for the tested mantle pressures and temperatures are known. Therefore, in this work, we use a method of heterophase equilibrium calculation based on the minimization of thermodynamic potentials [49].

The model [6] is based on the scheme of a multi-reservoir flow reactor: frontal convective lithospheric heating with the development of facial zoning of metasomatically changed lithospheric mantle [8], and filtering of magma gas in the permeable zone, while taking into account heat loss into the host rocks. For the less studied case of the permeable zone, the problem includes the following:

1. Supposed there is a magma source (appeared as a result of decompression melting in the convective mantle above a hot spot) with an upper boundary at the depths of 100–150 km (Figure 2).
2. From the magma source, magma fluid of $T = 1300\text{ }^\circ\text{C}$ flows into a permeable flat homogeneous zone having a 4 km width and vertically varying permeability and porosity, with a constant discharge and under the pressure P_{lit} ; the composition of the fluid (by the independent components R_0) is given in s (SP1, Table S1).
3. The phases of the heterophase fluid flow, which consists of a mixture of ideal gases separating from the upper mantle magma source, interact in the permeable zone.
4. This fluid flow forms heat, and the ‘physicochemical wave’ of temperature and mantle rock compositions changes.
5. The hydrodynamics of the thermal interaction are described using the two-velocity approximation, taking into account thermal losses into side rocks [50].

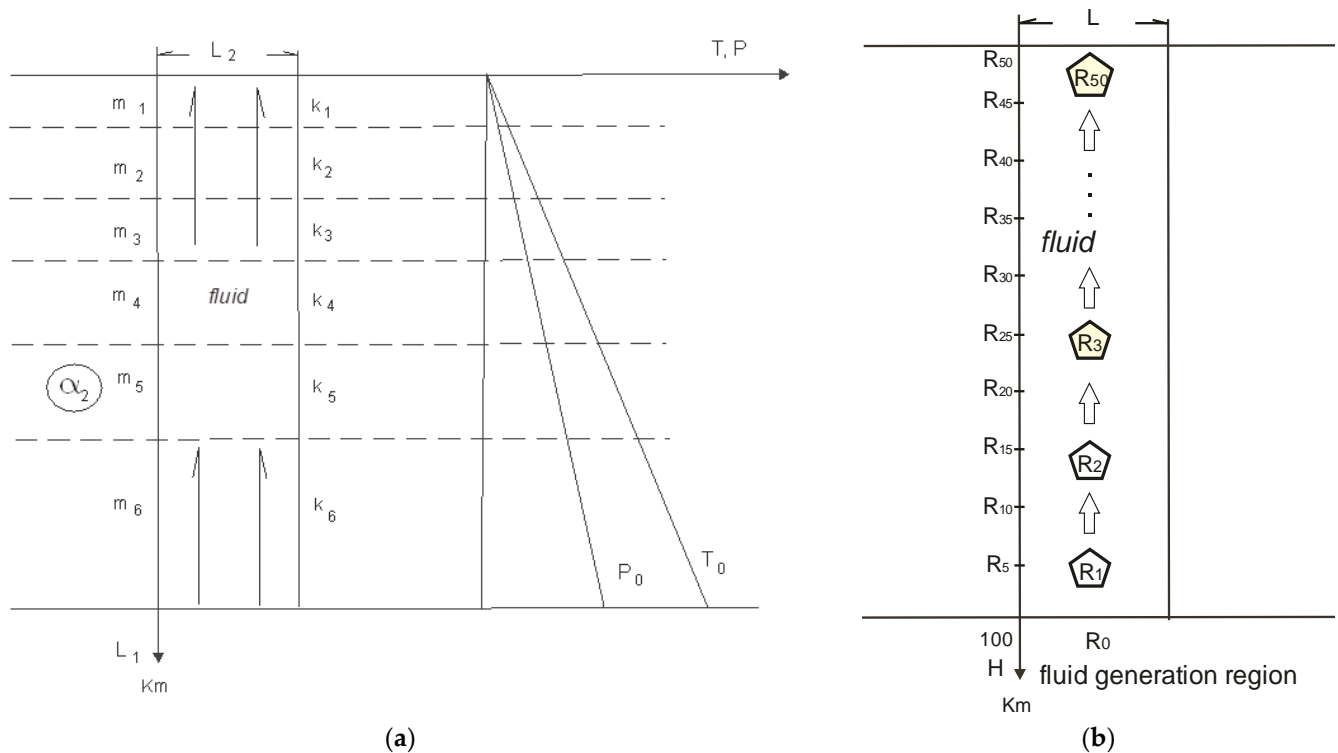


Figure 2. (a) Structural scheme of an over-asthenosphere permeable zone (‘fault’) of depth L_1 and width L_2 , with intersecting layered lithosphere of permeability k and porosity m (for separate layers); initial temperature and pressure distributions are T_0 and P_0 , respectively; and lateral heat loss by magmatogenic fluid flow is α_2 . (b) Scheme of the reactors’ distribution along the permeable zone.

We used the equations of physicochemical dynamics of metasomatic transformation for lithospheric mantle rocks, based on the model of heterophase ‘fluid-rock’ interaction, in the framework of two-velocity hydrodynamic models. One of the most effective methods to perform this is to use the law of conservation [51]. This method is based on major thermodynamics principles, conservation laws, and group invariance of the equations; this ensures that thermodynamically consistent dynamic models of heterophase media are obtained [52,53]. We consider a model with a two-phase medium consisting of rock and fluid (in the equations, the indexes $n = 1, 2$ are used, respectively) having partial densities ρ_n , velocities of melt/fluid percolations v_n , and specific entropy s [52,53]. The system of the governing equations includes the equation of continuity, the equation of phase movement, and the equation of entropy:

$$\frac{\partial \rho_n}{\partial t} + \text{div}(\rho_n v_n) = 0, \tag{1}$$

$$\frac{\partial v_n}{\partial t} + (v_n, \nabla)v_n = -\frac{1}{\rho}\nabla P - (-1)^n \frac{\rho - \rho_n}{\rho} \nabla Q + (-1)^n \frac{1}{\rho_n} \nu \nabla T + (-1)^n \frac{\rho_2}{\rho_n} b(v_1 - v_2) + \frac{1}{\rho_n} \partial_k(\eta_n v_{n,ik}) + g \quad (2)$$

$$\rho \frac{\partial s}{\partial t} + (j, \nabla)s = \kappa \frac{1}{T} \Delta T + \frac{1}{T} 2\nu(\nabla T, (v_1 - v_2)) + \frac{1}{T} \rho_2 b(v_1 - v_2)^2 + -\lambda(T - T_s) + \frac{1}{T} (\eta_1 v_{1,ik}^2 + \eta_2 v_{2,ik}^2) \quad (3)$$

Here, t is the time; T is the temperature; P is the pressure; Q is the parameter of the interphase interaction, which is determined by the pressure differences in the phases; ϕ is the porosity of the fluid-feeding rock conduits; ρ_2^{ph} and ρ_1^{ph} are the magma fluid and rock densities; $\rho_2 = \phi \rho_2^{ph}$ and $\rho_1 = (1 - \phi) \rho_1^{ph}$; $\rho = \rho_1 + \rho_2$ is the complete density; $j = \rho_1 v_1 + \rho_2 v_2$ is the complete impulse for the two-velocity medium; $v_{n, ik}$ is the velocity gradient tensor of phase n : $v_{n, ik} = \frac{1}{2}(\partial_k v_{n, i} + \partial_i v_{n, k} - \frac{2}{3} \delta_{ik} \text{div } v_n)$; $b = \eta_2 / \rho_2 k_p$ is the coefficient of interphase friction; k_p is the permeability coefficient for the fluid-feeding rock conduits; η_n is the dynamic viscosity coefficient of the phases; $\kappa = (1 - \phi) \kappa_1 + \phi \kappa_2$ is thermal capacity of the two-phase medium, with κ_2 and κ_1 being the thermal capacities of the magma fluid and fluid-feeding rock conduit; and g is the gravity constant. Kinetic coefficients, such as phase dynamic viscosities, thermal capacity, and coefficient ν , are the functions of the thermodynamic parameters. Introducing an entropy to the system in the above-mentioned form is possible because we suggest that the transient time for local thermal equilibrium between the phases is negligible when compared to the relaxation time of the interphase pressure. Because of the assumptions concerning temperature and pressure relaxation times, the entropy and complete density of the given two-phase medium are determined only by the hydrodynamic pressure and temperature: $\delta s = \delta s(\delta T, \delta P)$ and $\delta \rho = \delta \rho(\delta P, \delta T)$. The partial densities of the phases also depend on the parameter of the interphase interaction Q : $\delta \rho_n = \delta \rho_n(\delta P, \delta Q, \delta T)$. The coefficients of the volume compression α_q , the thermal expansion β , and the specific thermal capacity c_p , which characterize the heterophase medium, can be regarded as additive by phase.

The numerical analysis of the non-linear thermodynamically consistent model of hydrodynamics can be carried out using the method of control volume (CVM) [54,55]. This method is based on the integral conservation laws for any given closed volume; this also allows us to construct a mathematical model and to obtain physically correct solutions for arbitrary spatial and time scales of the studied system (provided the use of a completely implicit difference scheme). One of the problems of CVM is the calculation of the pressure field. The numerical solution for the equations of two-velocity hydrodynamics (1–3) is complicated because of the presence of the second pressure in the equation of phase movement. To solve this problem, we modified the iterative algorithm, SIMPLE, to calculate the pressure field using pressure and velocity corrections. The resulting complex structured system of linear equations was solved by the adapted method of varying directions, which provides fast convergence of the iteration procedure for dense grids [56]. The analysis of the results of our numerical experiments based on the modeling of the dynamics of heat and mass exchange during fluid movement in rocks shows that it is necessary to take into account the processes of rock compressibility and deformation to ensure the stability of the difference algorithm.

Heterophase interaction within the model of the multi-reservoir flow reactor is estimated using minimization of the Gibbs potential [49]: for every time step of heat-mass transfer in porous medium for the current P-T values in the subsequent reactor chain the problem of heterophase equilibriums calculation is solved. Initial temperature distribution for the problem of rock convective heating in permeable zone was taken from data for the full lithosphere profile during asthenosphere zones formation [57–59]. The data on inclusion study in minerals of mantle rocks from xenoliths in kimberlites [7] were taken into account to calculate a convective temperature profile over the asthenosphere fluid source; for that varieties of fluid compositions of corresponding effective thermal capacities were studied, from water-carbon-acid to nitrogen-carbon-acid [60].

5. Numerical Modeling of the Dynamics of Rock Carbonatization and Wehrlitization in the Permeable Zones of the Lithospheric Mantle under the Siberan Craton over the Asthenosphere

The frontal process of lithospheric mantle change over the asthenosphere zones is probably characterized by a certain general zoning type that is defined by stable magmatic fluid flow composition. This flow is defined at the crystallization front determined by the upper solidus, separating the advection zone consisting from the heterophases within the partially melted upper mantle [59]. The type of metasomatic zoning for lithospheric mantle, when fluid composition varies for the independent components in the system C-H-O (\pm S, N, Cl, and F), with a quasi-stationary temperature, and its distribution is shown in Figure 3. More permeable zones of the lithospheric mantle (where magma melts move) have a wider variety of metasomatic changes, both within the lower lithospheric boundary and in various depth facies [1,2]; this is proven by previous study on xenoliths in basalts, kimberlites, and multiphase-zoning carbonatite complexes [61,62]. Therefore, in this work, we take into account the dynamics of temperature changes with a wide variety of independent components in magma fluid: C-H-O-S-N-Cl-F (\pm Si, Ca, Fe, Al, Ti, Cr, Na, and K). The described model allows us better to understand the physicochemical conditions during the metasomatic changes in primary depleted lithospheric mantle matrix under influence of plume melts. This interaction created in turn kimberlite and basic and ultrabasic magmas (forming different-age magma complexes in the considered part of the Asian continental plate). In this case, it is necessary to understand how the substrates that produced carbonatite and tholeiitic melts of various compositions appeared.

5.1. Petrogenetic Aspects of Carbonatization and Other Metasomatic Changes of Depleted Rocks in the Lithospheric Mantle Profile

Comprehensive rock profiles of the lithospheric mantle under the SC and a continental plate of Central Asia were first described (based on a study of deep inclusions in intraplate igneous rocks) in 'Deep Xenoliths' [62]. Later further research was conducted on separate plate regions [2,20,46,61,63,64]. Shirey completed a study on mineralogical diamond associations with lithospheric mantle minerals for garnet diamond-bearing facies of the lithospheric mantle [65].

The comparative analyses of xenolith compositions in basic volcanogenic and kimberlitic rocks described in the above-mentioned publications show their substantial differences, both in-depth facies of their mineralogical associations and in their rock compositions. Mantle xenoliths in basalts (1) including metasomatized xenoliths are represented practically only by ultrabasic rocks of spinel and garnet facies related to the graphite stability zone and their metasomatic changes are manifested as interstitial changes and vein-shaped mica, including amphibole, pyroxene, and garnet aggregates. In kimberlites (2) a similar set of fragments for graphite sub-facies of carbon, but it is completed by specific rocks regarded as 'eclogites' [66]. This classification of diamond-bearing substrates of the lithospheric mantle and their classifications was done in S. Shirey's review [65]. The comparison of xenolith associations in basalts and kimberlites shows that near the asthenosphere boundary, lithospheric mantle rocks undergo to metasomatic changes, causing the formation of new garnets, ranging from almandine-grossular to chromium pyrope, while reduction-oxidation conditions change substantially. Near the lithosphere base growing diamonds may trap chromite, corundum, ilmenite, and native iron and sulfides together with silicates [65–71]. The thermodynamic conditions for the evolution of intraplate magma systems (shown on the T-P scheme and corresponding to certain rock associations) [5] allow us to suggest the existence of a structure with at least two zones for the metasomatic transformations of depleted rocks of the lithospheric mantle under the influence of magma fluids. Deep Ti-bearing cumulative 'eclogites' are formed in the lower part of the lithosphere [71], while the wehrlitization zones and other relatively low pressure–temperature processes involved in the metasomatic changes of ultrabasic lithospheric mantle are located above at several levels

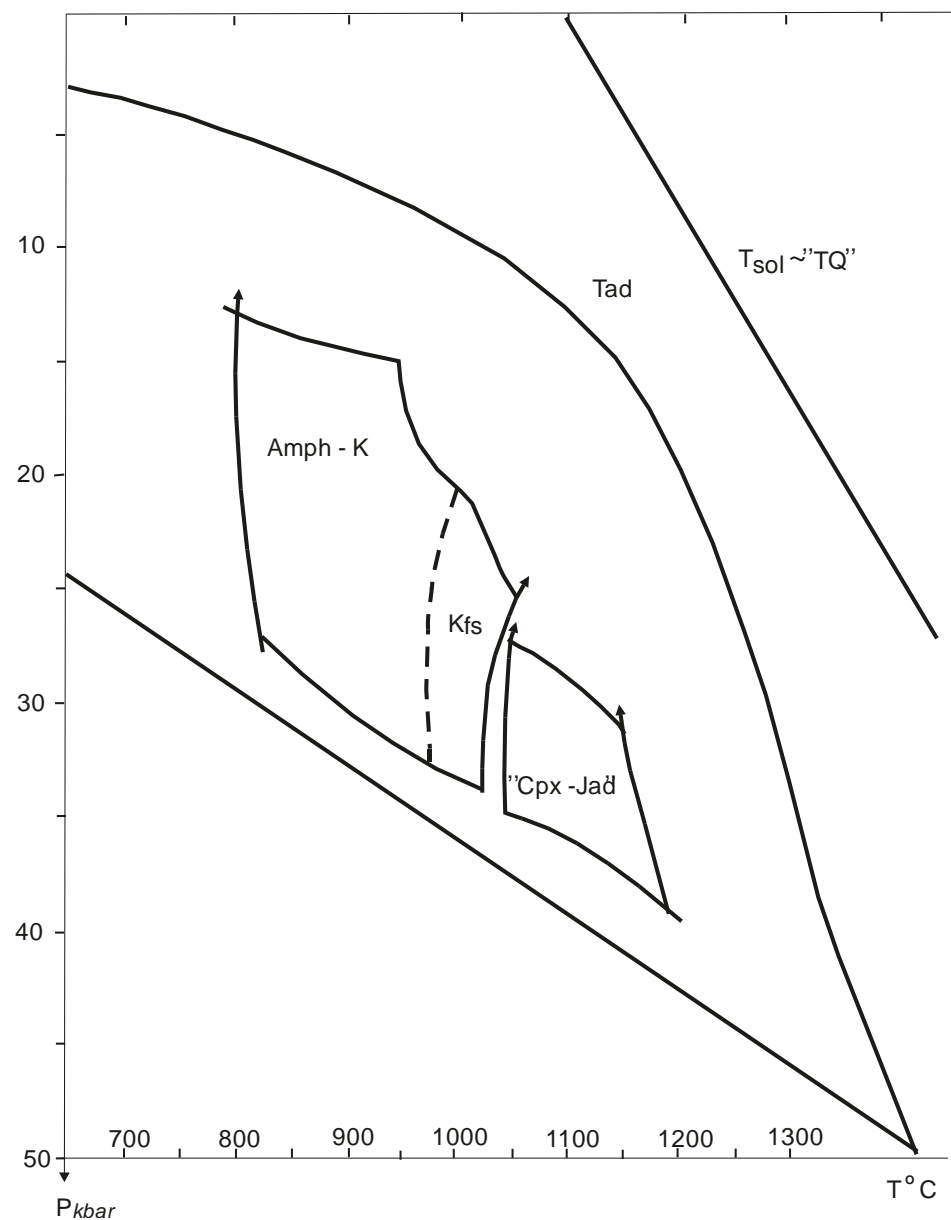


Figure 3. The formation of a two-zone structure: the appearance of a lower zone, where there is a local redistribution of ‘slowly mobile’ petrogenic components (Ca and Mg); somewhat larger displacements of Ti, Si, and Fe; a significant redistribution of Na; and complete depletion of rocks in terms of Mn, K, and P, and the development of an upper zone with potassium enrichment in metasomatized rocks. Amph-K is monoclinic potassium amphibole; Kfs is potassium feldspar; Cpx-Jad is monoclinic pyroxene with a high content of jadeite ‘molecule’; Tad is the adiabatic temperature; T sol is the solidus temperature for the ‘TQ’ substrate.

From the viewpoint of the theory of dynamics of non-isothermal metasomatism and taking into account the kinetics of major types of heterophase replacement reactions in the earth crust [48] (including the processes of granitization with convective melting of metasomatic rocks), the process of non-isothermal transformation of rock substrates is accompanied by the appearance of zonal metasomatic rocks having either distinct or gradual boundaries between the zones.

The considered processes of transformation of depleted ultrabasic rocks of the lithospheric mantle under the SP cratons can be classified into those similar to the granitization of earth’s crust layers. The similarity lies in the fact that the main physicochemical reaction

of these heterophase processes is the debasification of rocks containing a magma chamber. According to White [72], ultrabasic highly depleted rocks of the lithospheric mantle acquire new mineral composition; the melting of these rocks results in the appearance of basic fusions. According to the above-mentioned data on xenolith compositions for lithospheric mantle rocks and diamond inclusions, there are the following trends in the metasomatic transformations of ultrabasic rocks: (A) carbonatization with calcined and salinated grosspydite as the final product, and (B) wehrlitization of deeply depleted ultrabasic rock with pyroxenite as a final product. The crust analog of these processes is rhodizingeneization of serpentinites or serpentinized dunites. In other words, what is regarded as 'eclogites' [65] in the classification of diamond-bearing substrates is a natural primary zone of lithospheric mantle debasification, resulting in the carbonatization of ultrabasic substrate.

It is necessary to understand the process of 'eclogite' formation using the model of mantle metasomatism because of possible petrogenetic understanding of the above-mentioned classification of diamond-bearing substrates within the framework of thermo-mass exchange model; the history of the term 'eclogites' is also interesting. The discovery of xenoliths containing mostly grossular and diopside (they were called 'grosspydite') took place in the late 1950s, when metasomatism was not regarded as a cause of petrogenesis in the lithospheric mantle.

At that time, the appearance of pyroxene–garnet association in metamorphic petrology could be 'automatically' related only to the process of eclogitization. On the other hand, it was not clear from the primary rock substrates how these unusual compositions of garnets and associated minerals could appear during metamorphism in graphite and diamond sub-facies with carbon polymorphic modification.

We are not planning to discuss the validity of this hypothesis in this work. However, by studying the processes of mantle substrate petrogenesis based on the model of metasomatism, we should cover all the research on these processes in the contact zones between intrusive and host ultrabasic rocks [73–79]. These studies describe rodingites that are similar in composition to the mineral associations of grosspydites. Therefore, the analogy between crust and mantle processes of ultrabasic rock transformation by magma fluid is natural.

We believe that if rocks having the compositions of grosspydites or carbonatites appear deeper than the basic magma melting level, they can be regarded as the manifestations of deep rodingeneization of ultrabasic rocks. This idea concerns the analysis of mass equilibrium to find out changes in the petrogenetic components of the harzburgite, websterite, and tholeiite rock series (Figure 4). This example is important because tholeiites appeared as melts from lithospheric mantle during the development of the most voluminous intraplate magmatism in the geological history of the Asian continent. It is clear that the composition of metasomatized lithospheric substrate was replaced by harzburgite, and having a tholeiitic composition can appear when we replace $\approx 88\%$ of Mg with Si, Al, Ca, Na, Ti, and K. In this case, a simple process of wehrlitization of a depleted ultrabasic substrate can 'ensure' only an increase in Si and partly Ca contents in the formed metasomatites. The appearance of a metasomatic substrate with a composition 'suitable' to form tholeiitic melt should be followed by the formation of necessary and sufficient minerals containing Al and alkali metals.

Within the framework of the proposed approximation, there are certain physicochemical trends imitating the processes of ultrabasic rock transformation into zonal mineral associations of the above-mentioned type. In this case, if the obtained spatial metasomatic sequences of the mineral associations in our models are similar to the compositional variations in xenoliths the supposed model may be regarded as reasonable petrogenetic hypothesis.

This refer also to the mineral associations in xenoliths from kimberlites, as well as metasomatites in the xenoliths of ultrabasites from basalts. This may be reasonable hypothesis of the nature of grosspydite 'eclogites' as the analogues of crust rodingites. This may explain the variation in mineral inclusions in diamond.

The results of the numerical experiments using the program complex Selector-C are presented in the table (SP1, file S1).

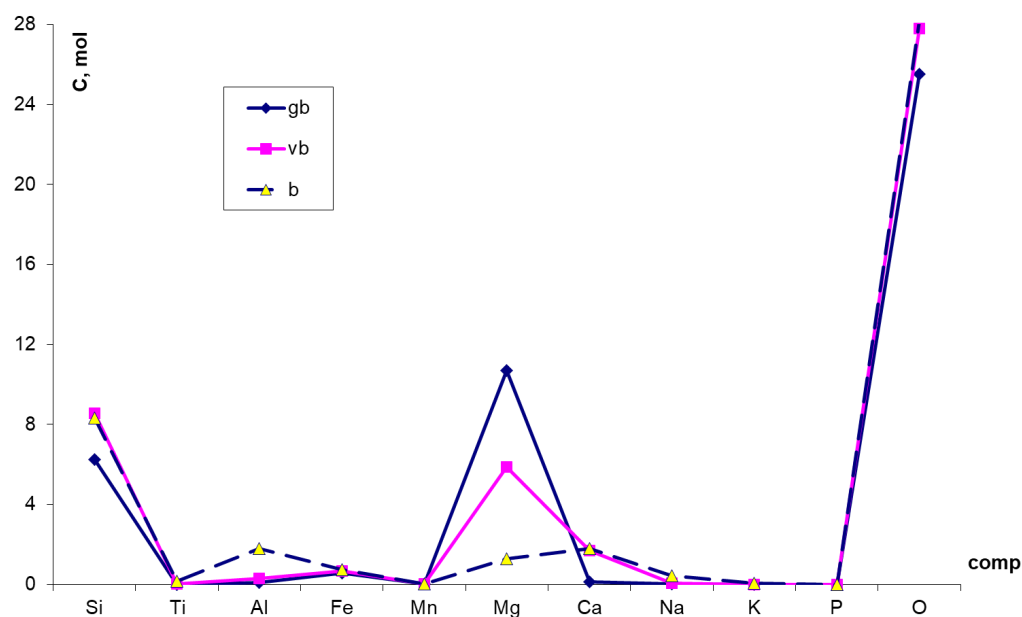


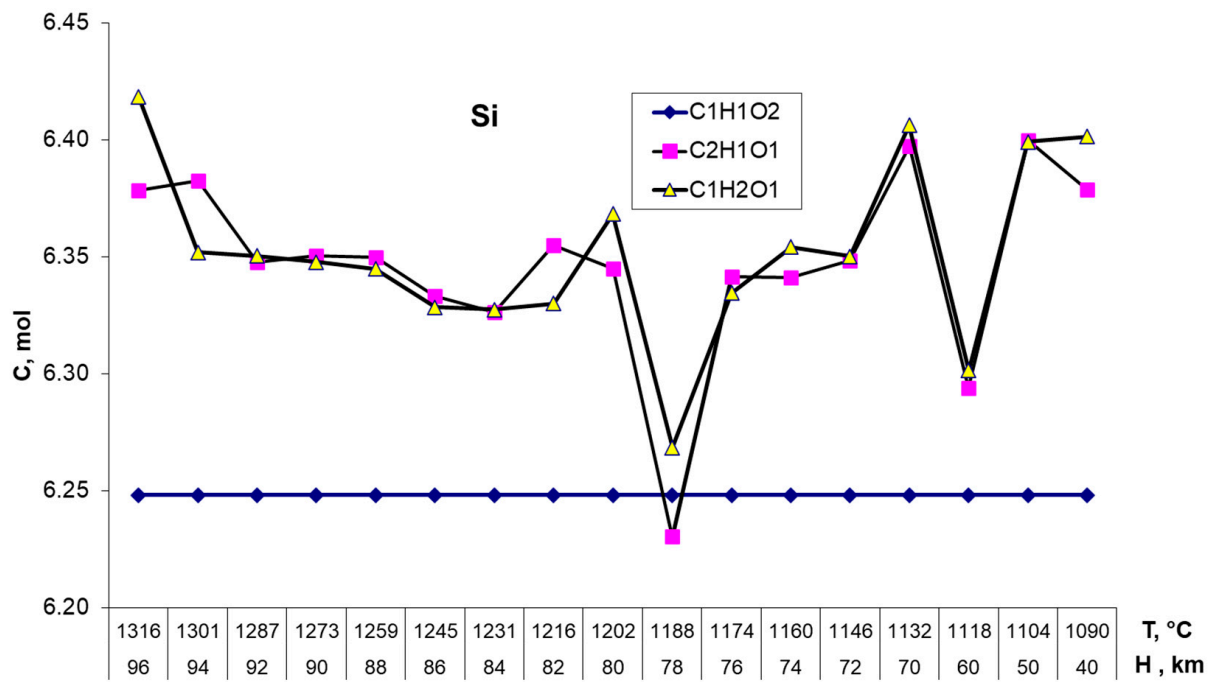
Figure 4. Mole content ratios of petrogenic components for the average compositions of harzburgite, websterite, and tholeiite.

5.2. Analysis of Physicochemical Factors Causing Various Zoning-Type Structures of Metasomatic Columns in Transformed Lithospheric Mantle Rocks

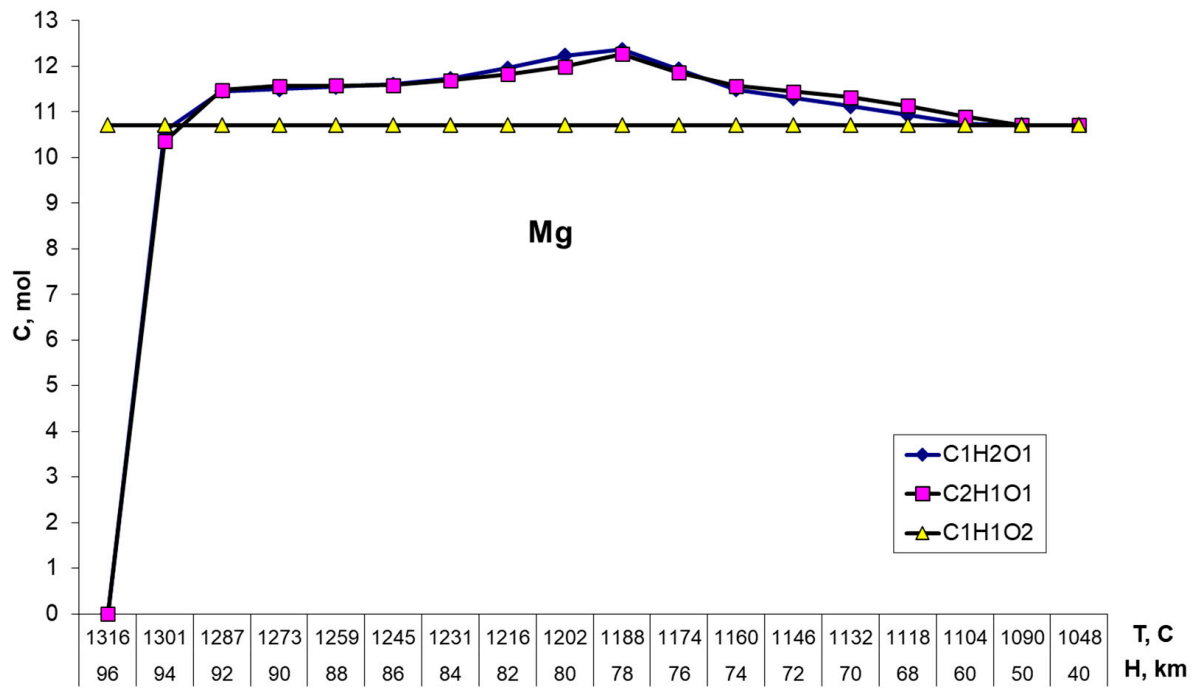
If there are metasomatic columns in the permeable fault zones over the asthenosphere magma chambers, they should contain several reactional mineral zones with the mineralogical associations represented by ultrabasic xenoliths, gnospydites, and other ‘eclogite’ associations [66], as well as metasomatic veined xenoliths [63,80,81]. This could be clearly understood if we compare with the homogeneous composition in harzburgite mantle substrate beneath the oceans. The problem may be solved suggesting the subsequent complication of the composition of magma fluids penetrating into the permeable zone from the magma chamber: (1) N; (2) C-H-O; (3) C-H-O-Cl-F; (4) C-H-O-Cl-F-N-S; (5) C-H-O-Cl-F-N-S-Si-Ca; and (6) C-H-O-Cl-F-N-S-Si-Ca-Al-Fe-Ti-Na-K.

We obtained the following results from the numerical experiments using the model of the flow reactor (using the above-mentioned compositions):

- (1) The virtual changes in the initial distribution of some petrogenic components in the homogeneous harzburgite substrate of the lithospheric mantle (under the influence of the above-mentioned fluids) have one common property—redistribution of most petrogenic components.
- (2) For most of the studied variations in the primary fluid compositions, there is a peculiar feature of the spatial redistribution for petrogenic components during the metasomatism of the harzburgite mantle substrate—‘noncoincidence’ of spatial and temperature locations for depleted and enrichment zones for rocks that are transformed by petrogenic components (Figure 5a–c);
- (3) All metasomatic columns for the quasi-stationary P and T profiles have at least four-zoning mineral structures for the mineral association distribution and the extent of ultrabasic substrate transformation, along with the lithospheric mantle profile (Figure 6).



(a)



(b)

Figure 5. Cont.

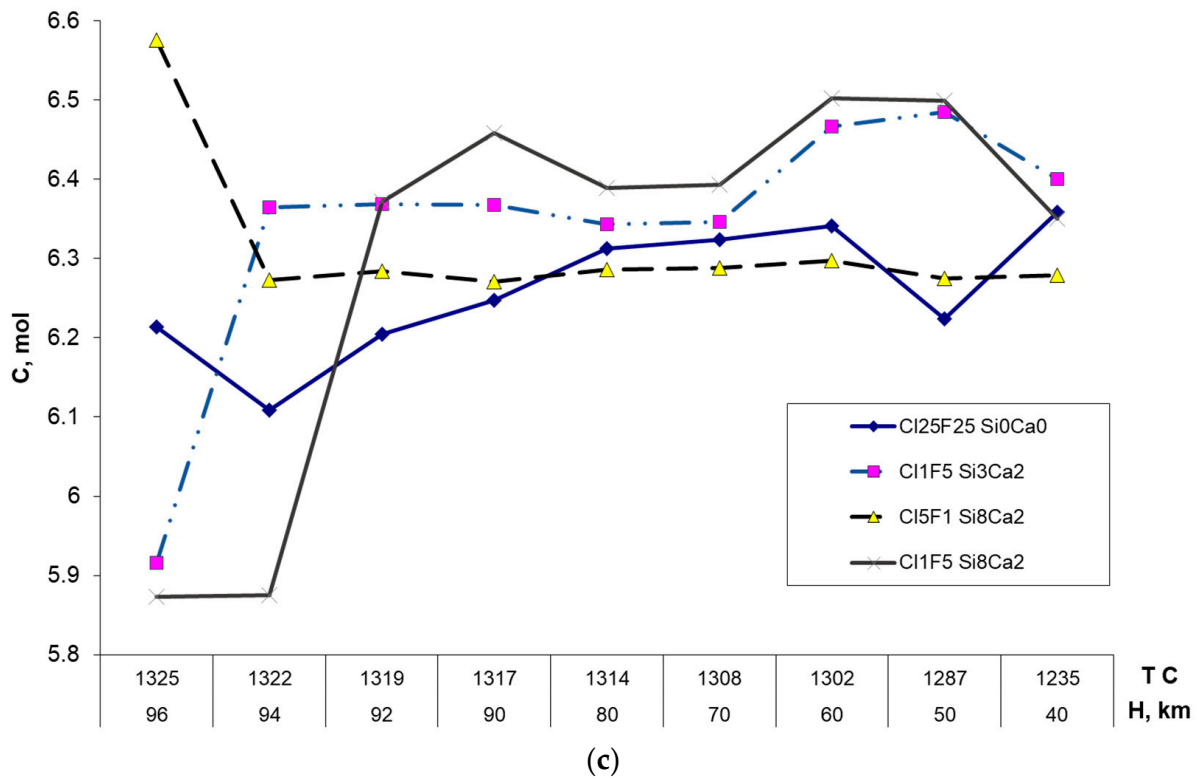


Figure 5. Distributions of elements in the permeable zone along the profile of ‘harzburgite’ lithospheric mantle after the influence of fluids: $t = 50,000$ thousand years, $K_p = 10^{-15} \text{ m}^2\text{--}10^{-13} \text{ m}^2$, and $m = 0.01\text{--}0.03$. Element distributions: (a) Si; (b) Mg; and (c) Si.

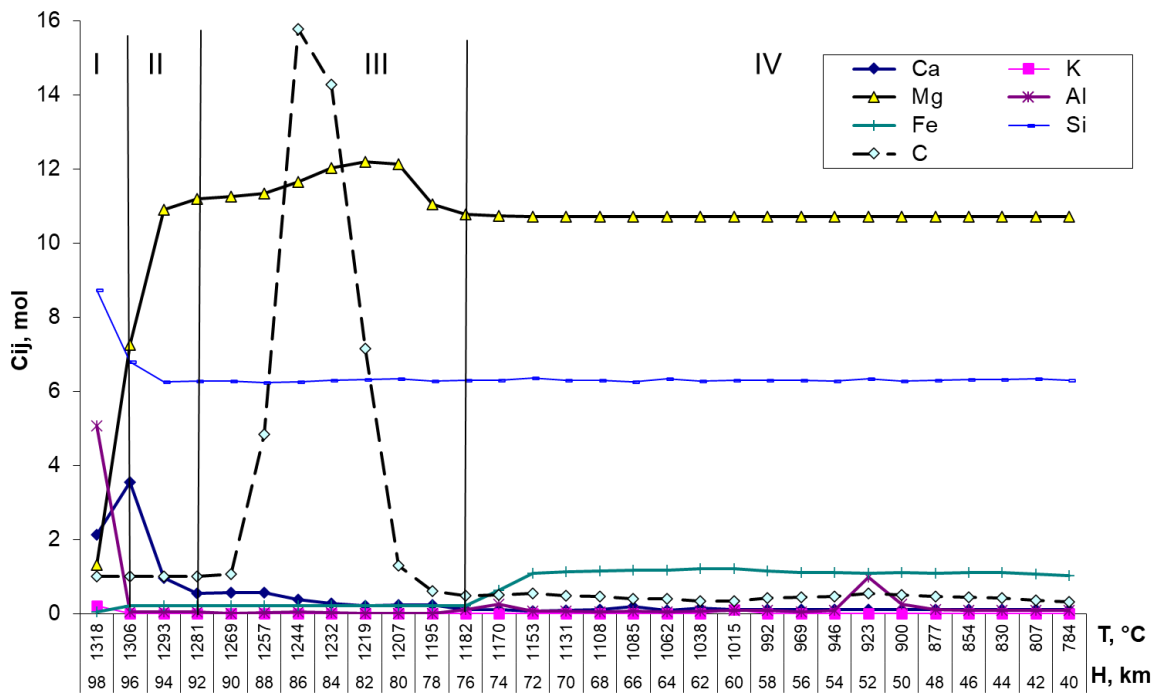


Figure 6. Zoning of petrogenic components’ distribution (zones I, II, III, and IV) along the metasomatic column after the influence of fluid composition: Si(0.8), Al(0.3), Ti(0.01), Fe(0.2), Ca(0.3), Na(0.04), K(0.02), Cl(0.5), F(0.1), C(1), H(2), and O(3).

As for the imitation of possible compositions of metasomatic substrates, which could be 'parental' for the intraplate magma systems, their flowing characteristics seem to be the most important: (1) a necessary manifestation for directed change in the mineral compositions of the zones, and (2) a suitable scale of debasification of the primary ultrabasic substrate. A decrease in olivine content during the formation of a new mineral association is a mineral characteristic of this substrate.

5.3. Physicochemical Conditions of Carbonatization for Lithospheric Mantle Rocks

Local and regional varieties in the compositions of Perm-Triassic SP melts are described by [32]. For the northern and north-western boundaries of the Siberian craton with lava sheet of the Putorana plateau and volcanic moulds of the northern part of the Siberian platform [82], the presence of a series of multiphase-zoning carbonatite massifs [61], where camaphorites (phoskorites) are mainly ore bearing, is typical [62]. As the above-mentioned works have shown, the standard sequence of their formation is realized through the appearance of the following intruding melt phases: dunites, melilites, pyroxenites, ijolites, nepheline syenites, phoskorites, calcium, and dolomite carbonatites. The nature of the formation of these types of intrusive bodies is rather disputable; however, in most recent publications authors agree that the preliminary metasomatic transformation of lithospheric mantle rocks by magmatogenic fluids coming from the magma chambers of the upper mantle [61,62] plays an important role. And the rock-melt/fluid interactions is the reason of the variations of mantle magmas and later different types of plutons. For these types of evolution of magma systems, a quantitative two-stage scheme has been proposed [83]:

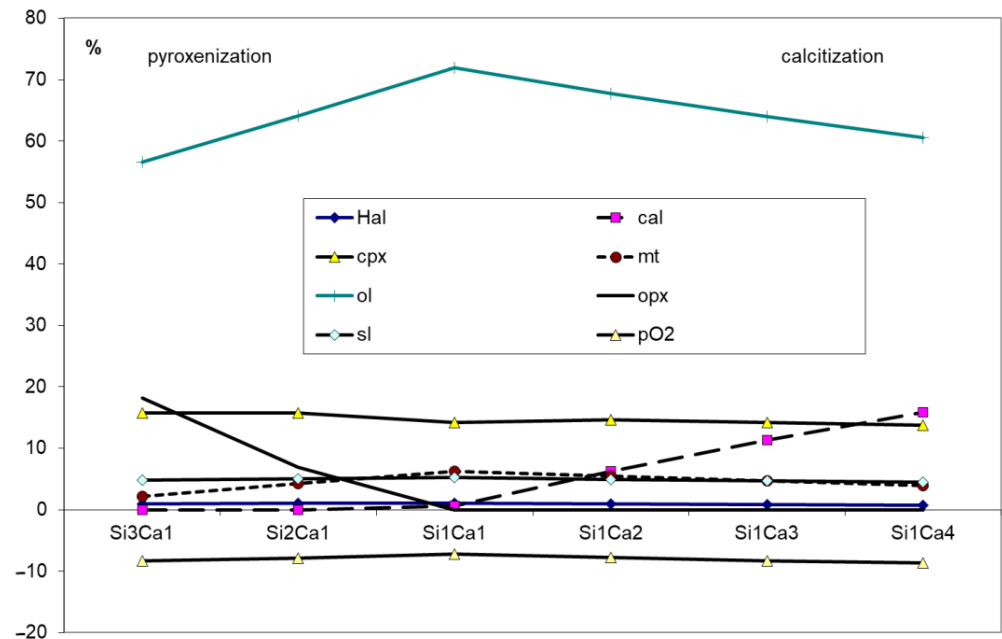
1. Metasomatic wehrlitization and carbonatization of mantle substrate.
2. Melting of metasomatically transformed substrate.

In this work, we consider the elements of physicochemical dynamics of the former stage of the given magma systems for the zone of carbonate-bearing associations of metasomatic rocks that forms at the lower boundary of the lithosphere plate.

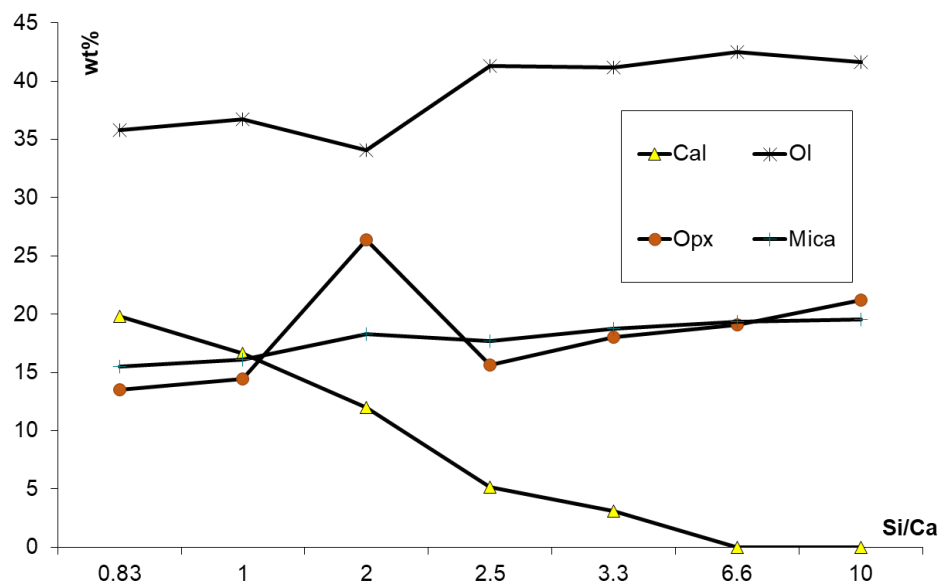
It is believed that the processes of the melting of magma to form SP carbonatite complexes are connected to magma forming due to metasomatic high-depleted substrates [61,62,83]. As earlier works on metasomatic transformation within the lower boundary of the lithospheric mantle show [58,59], the processes of carbonatization and salinization of rocks during metasomatism of lithospheric ultrabasites develop mostly in the lithosphere plate basement. We studied various types of homogeneous and layered profiles of the lithospheric mantle for the following ratios: C-H-O-S-N-Cl-F (\pm Si, Ca, Fe, Al, Ti, Cr, Na, and K). The petrogenetic influence of magma fluid flows is the most distinct for the deeply depleted harzburgite profile of the lithospheric mantle. This profile is also chosen because these rocks statistically prevail in mantle xenoliths. During the numerical modeling of metasomatic process in the approximation of the flow reactor (Figure 2), these changes were registered in reactors #1 and #2. Since P and T values in reactor #1 are practically constant, it is better to study the physicochemical transformations of the input composition of mantle rocks for this part of the system. In this case, the influence of individual components on the dynamics of metasomatism can be understood by fixing some component amounts and varying the others. It was found that the transient processes for the transformation of input mineral matrixes by stationary fluid flows (of weight amounts about 0.5–5% for reactor #1) do not last more than 10 thousand years, while permeability is 10^{-15} – 10^{-16} m². When permeability is more than 10^{-15} m², the time is about 3–5 thousand years.

According to existing geological data [61], the volume fraction of carbonatites in real intrusive complexes at the level of erosion sections of multiphase intrusions is about 10%, while dunite 'cores' compose 70%–80%; this is the second important factor for the solution of the problems related to the dynamics of metasomatism. Taking into account these data, we can conclude that the character and rate of metasomatic transformation of lithosphere substrates that produced these melts is close at least modal variations of minerals in metasomatic rocks.

In this case, in our physicochemical modeling, we can estimate the boundaries of the stability for calcite, pyroxene, etc., as well as their proportions in separate intrusive phases and fractions for the separate phases of carbonatite -ultramafic massifs [61]. To find the above-mentioned ratios, we assumed that both compositions of the gas phase and pO_2 of the heterophase system are defined mainly by the modular values of C, H, and O. The results of the numerical experiments are shown in Figures 7–10.



(a)



(b)

Figure 7. (a) Ratios for calcinations and wehrlitzation zones versus Si and Ca contents in magma fluid. (b) The boundary of calcination zone of harzburgite matrix versus Si and Ca contents in magma fluid.

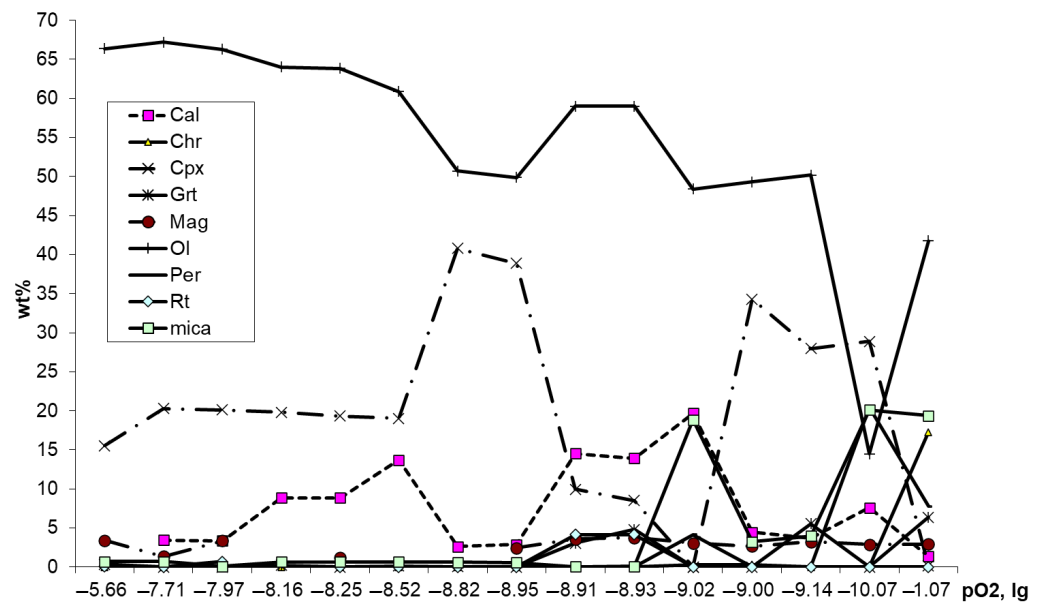


Figure 8. Composition of metasomatic mineral associations in zone I (Figure 6) versus pO_2 in magma fluid.

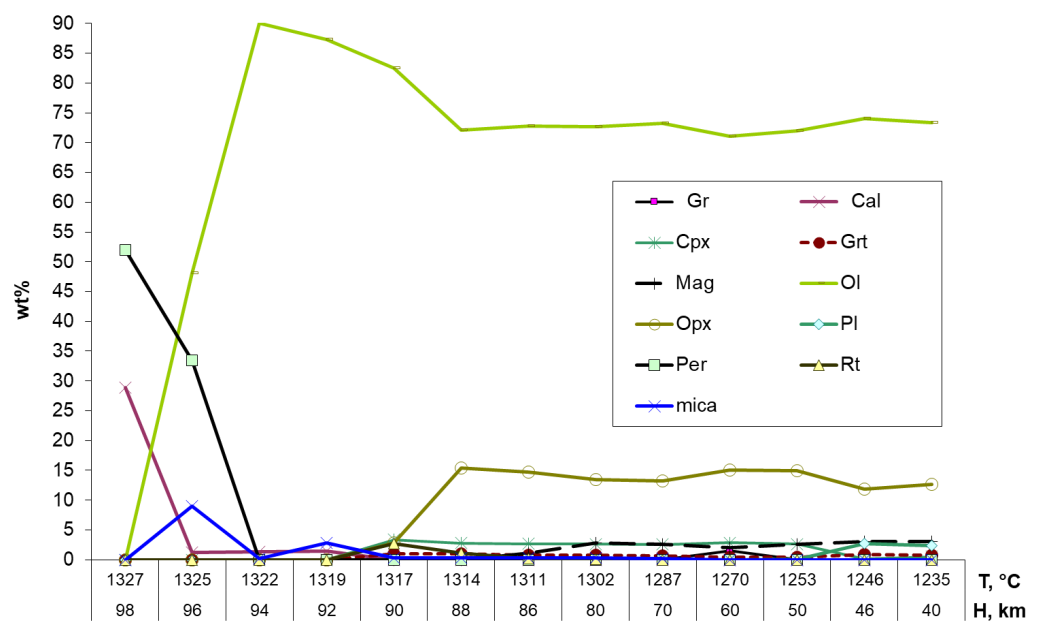


Figure 9. An example of intensive sublimation (dissolving) of petrogenic components in zone I (Figure 6) under the influence of magma fluids with low contents of petrogenic components; in this example, the fluid composition is C(1), H(2), O(3), Cl(0.5), F(0.1), Si(0.01), Al(0.01), Fe(0.01), and Ca(0.01).

An analysis of the obtained data shows that the characteristics of carbonatization and wehrlitization of highly depleted mantle substrates by asthenosphere magma fluids is defined by two aspects: (1) the ratios of C-H-O modules, and (2) the ratios of Si and Ca contents in the magmatogenic fluid. The process of carbonatization of dunite substrates for the given range of pO_2 variations and Si and Ca ratio contents in magmatogenic fluid can be characterized by the following features: (1) there are different zones of wehrlitization and calcitization (Figure 7a); (2) the zones of development of camaphorites and non-magnetite calcitization are different (Figure 7a); (3) there are also different zones for calcitization, garnet formation, and maximum rate of alkali metasomatism (Figure 7b); (4) wehrlitization

and calcitization are defined by various ratios of Si and Ca in the fluid phase (Figure 8); (5) the trend of dynamics for the metasomatic transformation of ultrabasic substrates depends on (under the same conditions) weight fraction of the fluid phase penetrating from the magma source (Figure 9); and (6) the analysis of the dependence between petrogenic component mobility and pO_2 shows that transfer of most petrogenic components from the reaction zone is the highest for the range $\lg pO_2 \approx -8 \div -8.9$ (Figure 10).

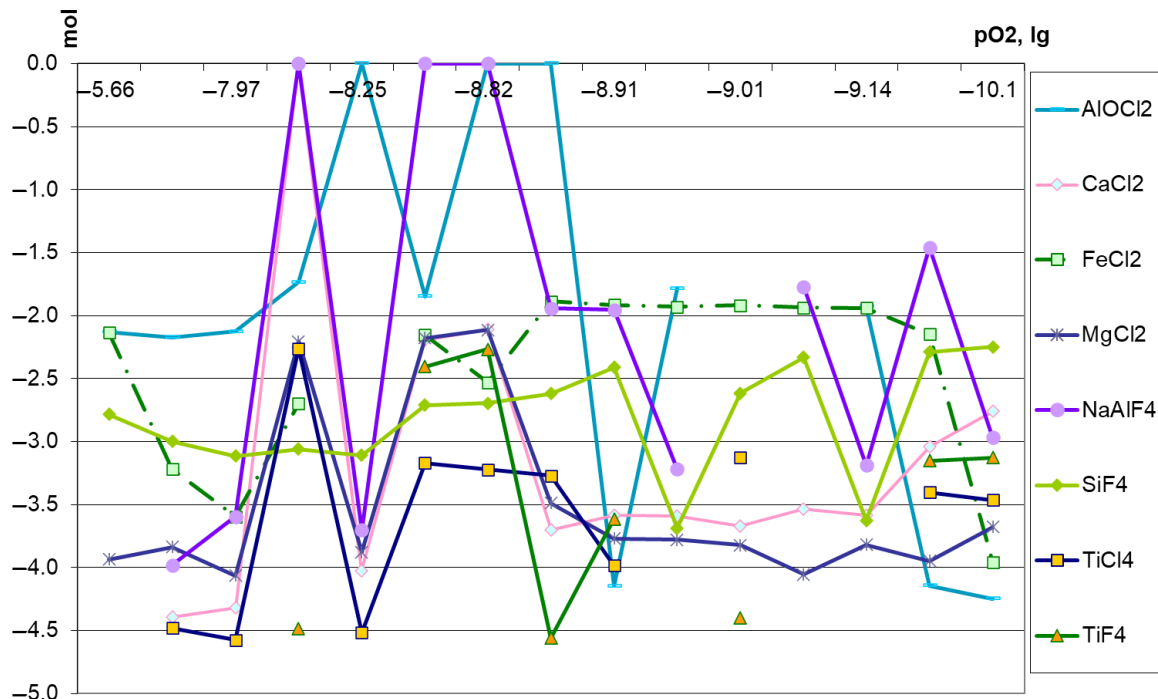


Figure 10. Quantities of gases transporting petrogenic components versus pO_2 value; the ratios are given by the C/H/O modules in magma fluids containing Si(0.1), Al(0.1), Fe(0.1), Ca(0.1), Cl(0.5), and F(0.1) in reactor R_0 .

5.4. Physicochemical Conditions for the Evolution of Grospydite and Other Mineral Associations with Garnet with a Complex Composition within the Lithospheric Mantle

If a calcitization zone in the metasomatic column is conjugated to the lower boundary of the lithosphere plate, according to composition variations in garnets and associating mineral complexes in xenoliths of ‘eclogites’ [66], the evolutions of garnets (covered in the above-mentioned publications) can cover a larger depth range compared to a carbonatization zone. As the above data show, the zone of grossular garnets is associated with a calcination zone for a certain range of variations in possible magma fluid compositions. However, metasomatic Ca- enriched garnets with complex compositions are found both in graphite and diamond sub-facies without appeared carbonization [66,80,81]. The manifestation of mineral associations with garnets of transitional compositions and varying contents of chrome and iron is accompanied by variations in the compositions and contents of both pyroxenes and accessory minerals. It is important that the garnet content in the rocks under consideration varies from $\approx 20\%$ to 80% in grospydites, and up to 19% – 20% in olivine-containing ultrabasic rocks [66]. The presence of disthene and corundum in grospydites shows that magmatogene fluids contain unusual component ratios. After sorting their compositions (SP1, Table S5), we found some combinations that are suitable to describe the above-mentioned features of mineral associations within the zones of metasomatic columns:

- (1) Within one metasomatic column, the formation of zones having maximum contents of grossular and pyrope is possible (Figure 11).

- (2) The formation of grossular garnet zone (associated with ferrous orthopyroxene, but not diopside) is possible; this zone is changed into the zone of diopside, and then, along with the lithosphere profile, into the zone of wehrlitized harzburgite with clino- and orthopyroxene sub-zones (Figure 12).
- (3) The formation of grosspydite–kyanite zone changed by the zone of practically monomineral diopsidite (Figure 13), followed by the zone of wehrlitization of harzburgite with the above-mentioned sub-zones.
- (4) The process of garnatization of the ultrabasic matrix (without the formation of associated pyroxenes) is possible (Figure 14).
- (5) The formation of subsequent zone of “garnatization” in the ultrabasic mantle does not essentially depend on the pressure variations along the permeable zone (Figure 15).

The role of certain physicochemical factors, determined from the given varieties, is shown in the tables presenting the data for the transition zone between grosspydite and wehrlites. The activities of the independent components (SP1, Tables S6–S9) mostly vary within the transition zone. A general analysis of the obtained data shows that associations of grosspydite type form at a certain range of C-H-O ratios with the following magma fluid composition: $C(1)H(1)O(2) \div C(0.5)H(0.5)O(1)$. In this case, andradite-grossular series with garnets could form only under the influence of reduced fluids, which not only do not produce iron sublimation from rock matrix, but add it to the formed metasomatic rocks. The appearance of a phlogopitization zone during convective heating and the metasomatism of the ultrabasic matrix can be virtually found at the temperature interval of 1000–1110 °C, for a depth range 120–40 km, when the fluid contains Cl < 0.3 moles and F of no more than 0.06 moles. Accessory chromite always appears beyond the garnatization zones, while escolaitite is typical for garnet-free calcinations zones at the oxygen potential range of $-7.0 > \lg pO_2 > -10.9$.

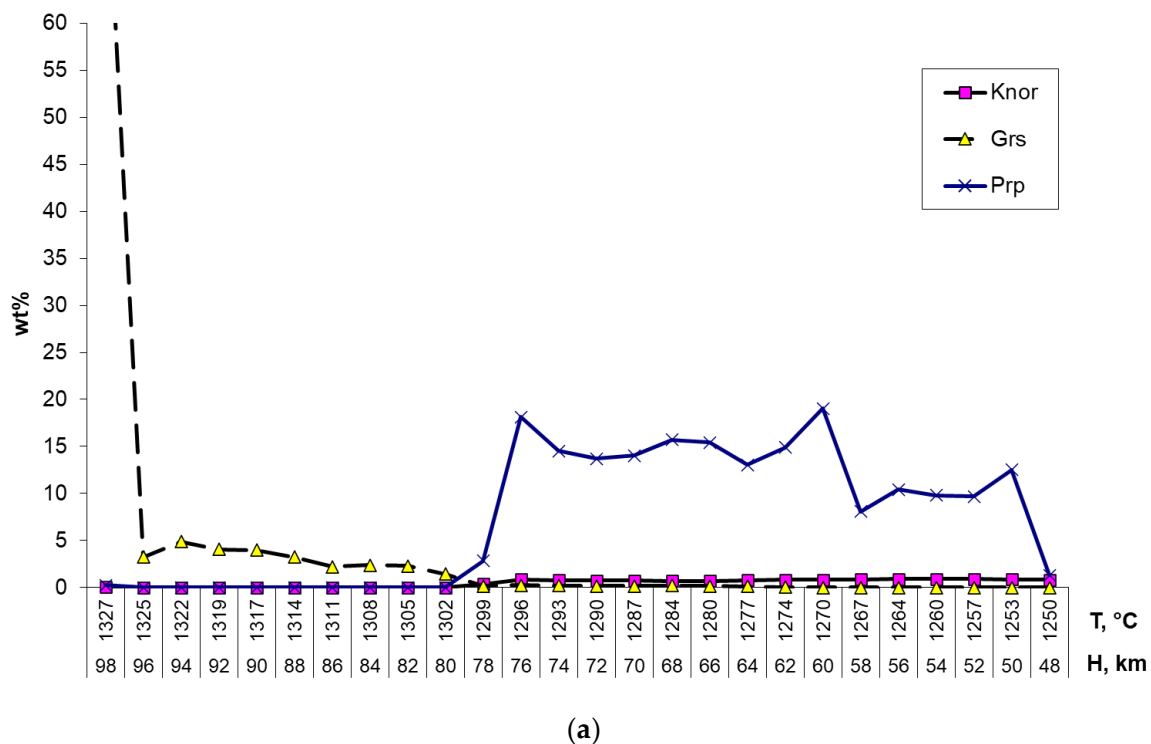


Figure 11. Cont.

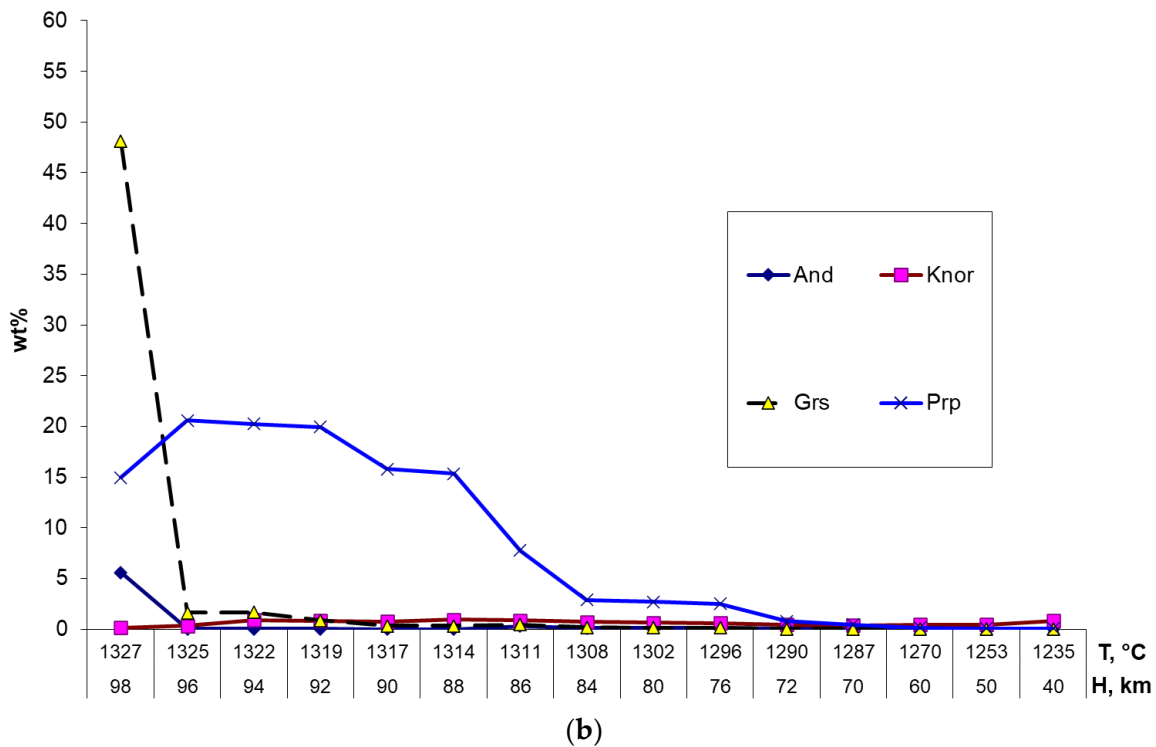


Figure 11. Distribution of garnets along the profile of a metasomatic column versus the composition of influencing fluid: (a) fluid composition is Si(0.6), Al(0.5), Ti(0.01), Fe(0.2), Ca(0.5), Na(0.04), K(0.01), Cl(0.8), F(0.2), C(1), H(2), and O(3), and (b) fluid composition is Si(0.4), Al(0.4), Ti(0.01), Fe(0.2), Ca(0.2), Na(0.04), K(0.01), Cl(0.5), F(0.1), C(1), H(2), and O(3).

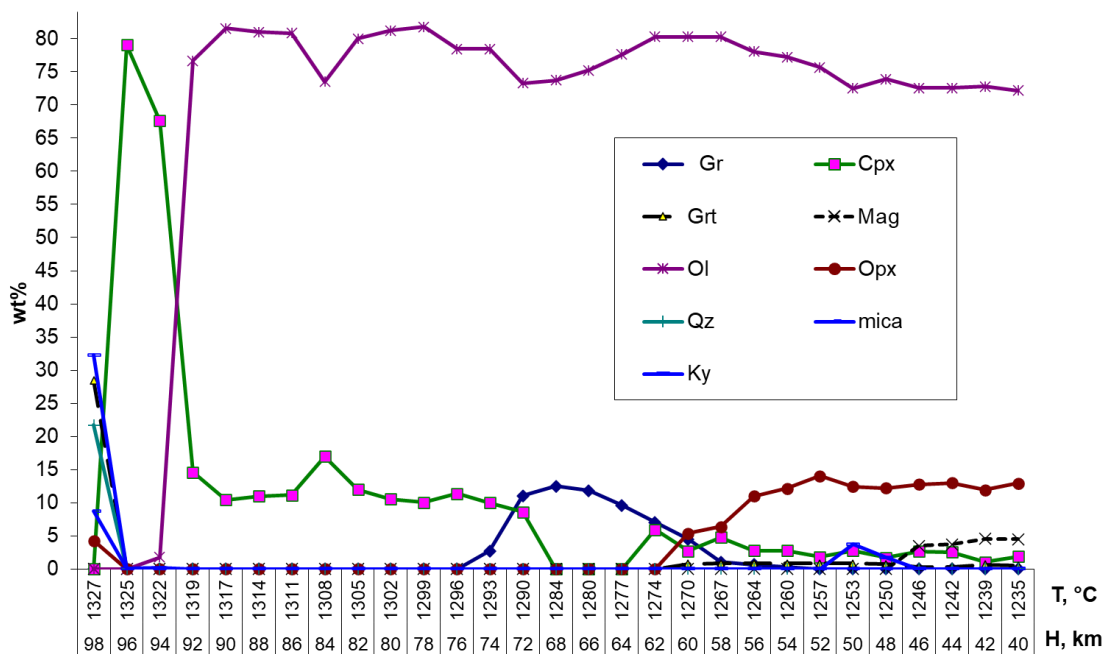


Figure 12. Formation of separate zones of wehrlitization, with kyanite and without kyanite: zone I: formation of rodingite with grossular, kyanite, and quartz with a low content of orthopyroxene; zone II: practically monomineral zone of diopside; and zone III: quasi-homogeneously wehrlitized ultrabasic rock changed by the zone of graphitized dunite and the by the zone of metasomatic ultrabasicite with low contents of kyanite and corundum.

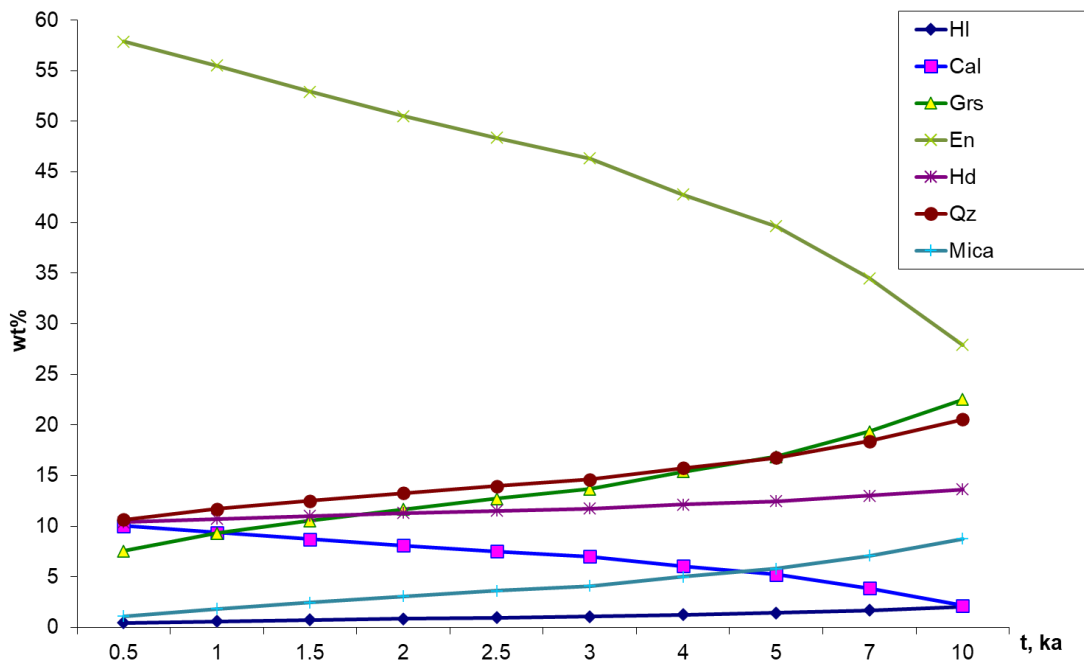


Figure 13. An example of the dynamics of formation of zone I: calcitized rodingite without diopside, under the influence of the fluid composition with Si(0.5), Al(0.1), Ti(0.01), Fe(0.1), Ca(0.5), Na(0.04), K(0.02), Cl(0.1), F(0.3), C(1), H(2), and O(3).

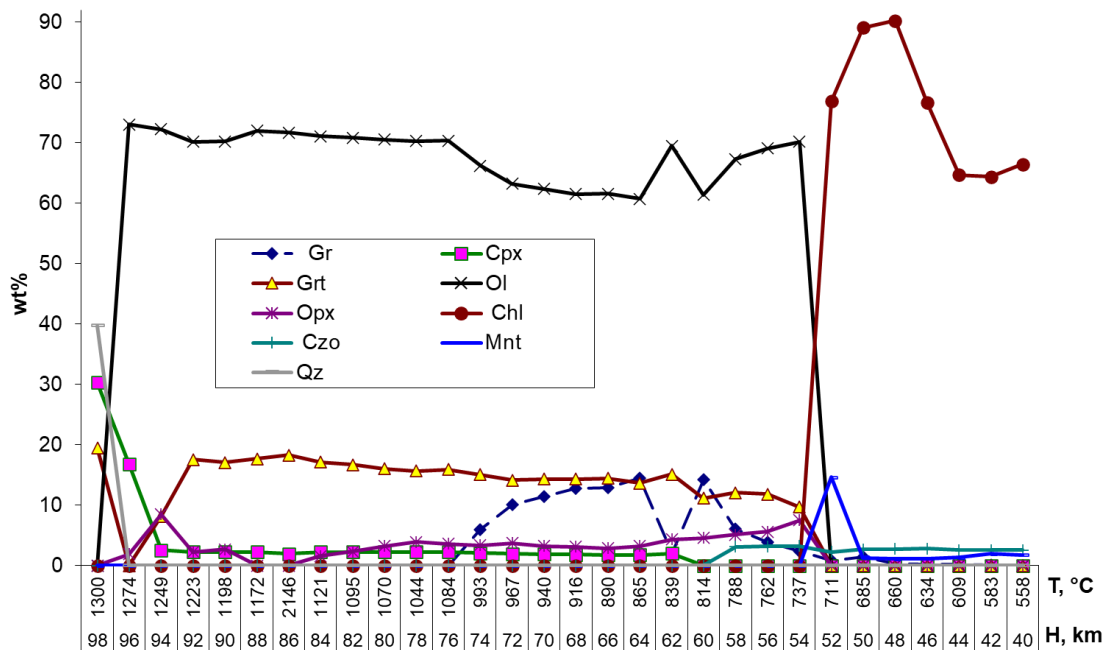


Figure 14. Mineralogical zoning in a metasomatic column (harzburgite matrix) under the influence of fluid composition with Si(0.8), Al(0.4), Ti(0.01), Fe(0.1), Ca(0.2), Na(0.03), K(0.02), Cl(0.5), F(0.1), C(1), H(2), and O(3). Structural parameters of the permeable zone: $K_p = 10^{-16} \text{ m}^2\text{--}10^{-13} \text{ m}^2$, $m = 0.01\text{--}0.03$, and influence time $t = 100$ thousand years.

In our numerical experiments, we did not obtain magnesite, sanidine, and native iron (which are found in diamond-bearing grospsydites and diamond inclusions along with other minerals [65,66]). The rather simple compositions of the obtained minerals can probably be explained by restriction of the thermodynamic data and the impossibility in estimating the contents of trace elements (Ni, Ca, Al, Na, Ti etc) in olivine ortho-, and clinopyroxene in our

numerical experiments. On the other hand, to solve the dynamic problem of convective thermo- and mass transfer in detail for the zones of deep faults draining the magma chambers in the upper mantle, an attempt to examine this in combination with the model of the flow reactor is presented below.

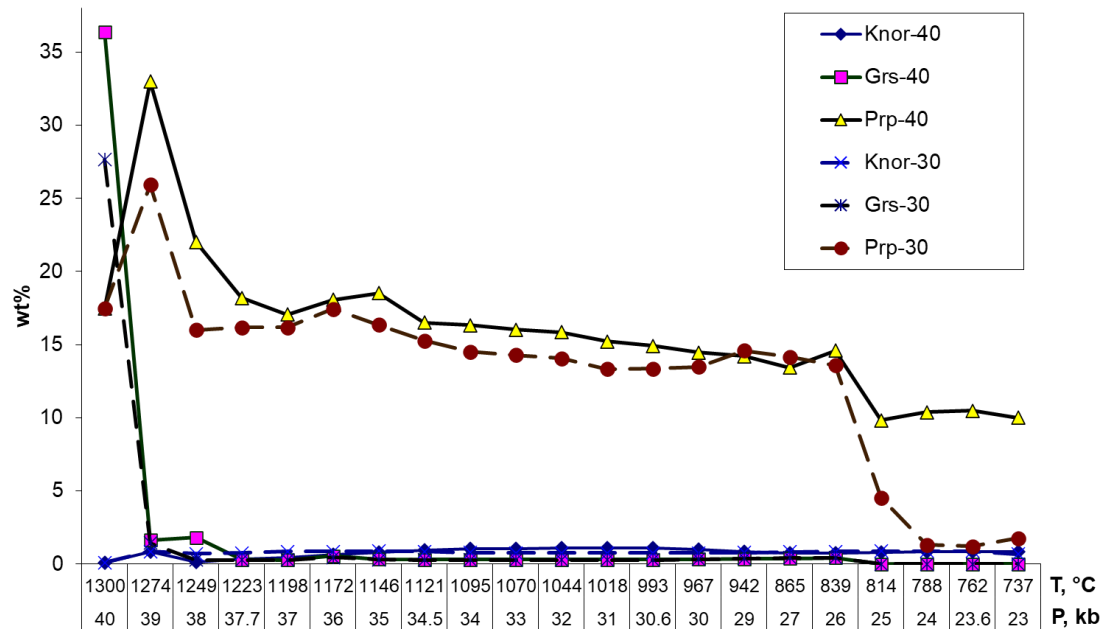


Figure 15. Garnet contents and compositions along the vertical profile of the permeable zone in the lithospheric mantle, as calculated for two profiles with various depths (superposition of two graphs): (1) lithosphere thickness is 150 km; T and P have linear stationary distributions, from 1300 °C and 40 kbar at the lower boundary of the system, up to zero values on the plate surface; and index '40' designates the minal contents in garnets; (2) the same conditions as in (1), with the lithosphere thickness of 100 km; T = 1300 °C and P = 30 kbar at the lower boundary; index '30' designates the minal contents in garnets; fluid composition: Si(0.8), Al(0.4), Ti(0.01), Fe(0.1), Ca(0.2), Na(0.03), K(0.02), Cl(0.5), F(0.1), C(1), H(2), and O(3).

6. Discussion

6.1. Implication for Natural Processes

The comparisons of the fluid inclusion compositions from different rocks brings us to the following general conclusions: (1) metamorphic rocks of the lower crust in the total gas phase substantially differ in amphibolite and granulite facies when compared to the gas phase in rocks from the fault zones of the lithospheric mantle; (2) it can be expected that the gas phase composition of some types of diamonds will differ from that in the major mineral (ol—olivine) of rock matrix; and (3) the quantity of stable clusters in all mineralogical groups of mantle rocks suggests that magmatogene fluids influence the mantle under the craton of the Udachnaya pipe.

The numerical modeling of the metasomatic dynamics of depleted upper-mantle substrates cover variations of mantle rock sequences. This can helps for the explanation for the nature of mantle magmas creating trap provinces in the SC and Siberian platform. The reasons for the variations in the composition of mantle fluid flows remain a subject for further research. Tectonic analysis of the Siberian platform suggest presence of global meridional fault zone served as conduits of mantle igneous systems. These works show meridional faults in which diamond-bearing igneous systems cyclically develop from the middle Paleozoic to the Mesozoic. The Maymecha-Kotui province with alkaline igneous rocks and zonal carbonatite intrusive bodies are located at the intersection of the aforementioned 'Rosen lineament' and latitudinal regional fault. Therefore, the compositions of mantle fluid flows beneath the SC should vary for the faults of different scales. Fluid

dynamics models have been used to describe common trap systems, including carbonatite and diamondiferous kimberlite manifestations under the SC. Determination of the physicochemical characteristics of the formation of common carbonatite substrates above the extinction areas of the upper-mantle tholeiite melting zones allows an examination of more complex dynamics of the formation of metasomatic transformations of depleted sites in upper-mantle rocks in diamond-bearing systems, for which sufficient statistical records of gas phase compositions and minerals of mantle xenoliths have been obtained.

According to the experimental study on metasomatic changes in mafic rocks at the common temperature range of the gas phase, which separates during the crystallization of trap melts in igneous upper-mantle and crust chambers, the characteristics of metasomatic changes significantly differ from those in the deep fluid systems shown above. The complexes which were created within the mantle columns subjected to the metasomatic changes may explain the variations of petrochemical magma compositions between the trap provinces of the SC.

6.2. Zones of Carbonatite Metasomatism within the Mantle Columns Beneath the Kimberlite Pipes according to the PT Modeling Using Mantle Xenocrysts and Xenolith

We made reconstructions of the lithospheric mantle using a series of monomineral thermobarometers [84,85] for garnets and ilmenites beneath the large kimberlite pipes in Daldyn and Alakit, and the kimberlite pipes Zarnitsa, Udachnaya, and Aykhal in Yakutia [86]). Here, we are mainly interested in garnet because the CaO level in clinopyroxene and in picroilmenites is significantly regulated by temperature, which can trace the proto-kimberlite evolution.

The most distinct maximum CaO is observed at the base of the lithospheric mantle at the level of 7 GPa. Here, the source of metasomatism is the proto-kimberlite melts that form a channel for subsequent melt intrusion. According to existing knowledge, such melts are essentially carbonatitic and have a very high temperature of ~1450 °C [87,88].

Another obvious level where there is substantial carbonate metasomatism is the area where the finishing of crystallization of proto-kimberlites is commonly at 4 GPa, when it becomes substantially carbonatitic [89].

In the case of a sharply layered lithosphere and a substantially stepped rise of proto-kimberlites, each level where the rise stops and the intermediate chambers are formed, with an example being the Zarnitsa pipe [90] (Ashchepkov et al., 2021), proto-kimberlites become a source of such metasomatism [91–96].

In addition, there is a level of wehrlitization that is significantly pronounced in many mantle columns at 3.5–1.5 GPa, which corresponds to the final evolution and crystallization of various mantle plumes with substantial carbonatite melts that come and stop at the upper boundary of the pyroxenite lens at 3.5–4.5 GPa in the middle part of the lithospheric mantle [93]. In ancient Archean times, this was the lower boundary of the lithosphere. This boundary has several physicochemical processes, including the beginning of a significant liquation of silicate carbonate magmas [88].

A slight jump in CaO in garnets is often manifested in a step at the garnet–spinel transition, which is the density boundary. Thus, any reasons for stopping melts usually lead to carbonatite metasomatism.

In ancient Archean times, the situation was somewhat different. According to the thermobarometry of inclusions in diamond, we observe trends with a gradual increase in the CaO level in garnets at separate 4–5 levels in the lower part of the lithospheric mantle from 8 to 4 GPa, which probably corresponds to the progressive metasomatism of significantly calcium-enriched subduction-related melts with dunites (Figure 16a–e). However, it may correspond to the primary bulk-rock variations.

For the Mir pipe, the situation differs because the ilmenite trend formed by protokimberlites is very long, starting from the lithosphere base to the Moho boundary. However, the degree of the interaction of protokimberlites was not high because there are no magnesium ilmenites marking typical for metasomatites, and thus, the interaction with these melts

before the eruptions was not pronounced. Pyroxenization in the middle part corresponding to the pyroxenite layer [31] and the upper part of the lithospheric mantle was probably caused by silicate melts long before the kimberlite stage.

Comparisons of the mantle columns of the studied pipes show significantly higher interaction of proto-kimberlites with the mantle column beneath the Zarnitsa pipe [88] when compared to the Aykhal and Udachnaya pipes. In Zarnitsa, many diamonds show high degrees of resorptions [99], possibly caused by carbonatitic melts [100]. In the Mir pipe, the dissolution of diamonds was not found, but two stage of their creation was detected [101], along with the growth of newly formed diamonds related to proto-kimberlites [102,103]. The mantle column beneath the Roberts Victor pipe from South Africa contains the most depleted CaO pyropes, (Figure 16e). There are only several levels with small CaO enrichment, including at the lithosphere base at 6 GPa and dipper at 7 GPa, at the level of Pyroxenite lens at 4 GPa, and near the garnet–spinel transition zone at 2 GPa.

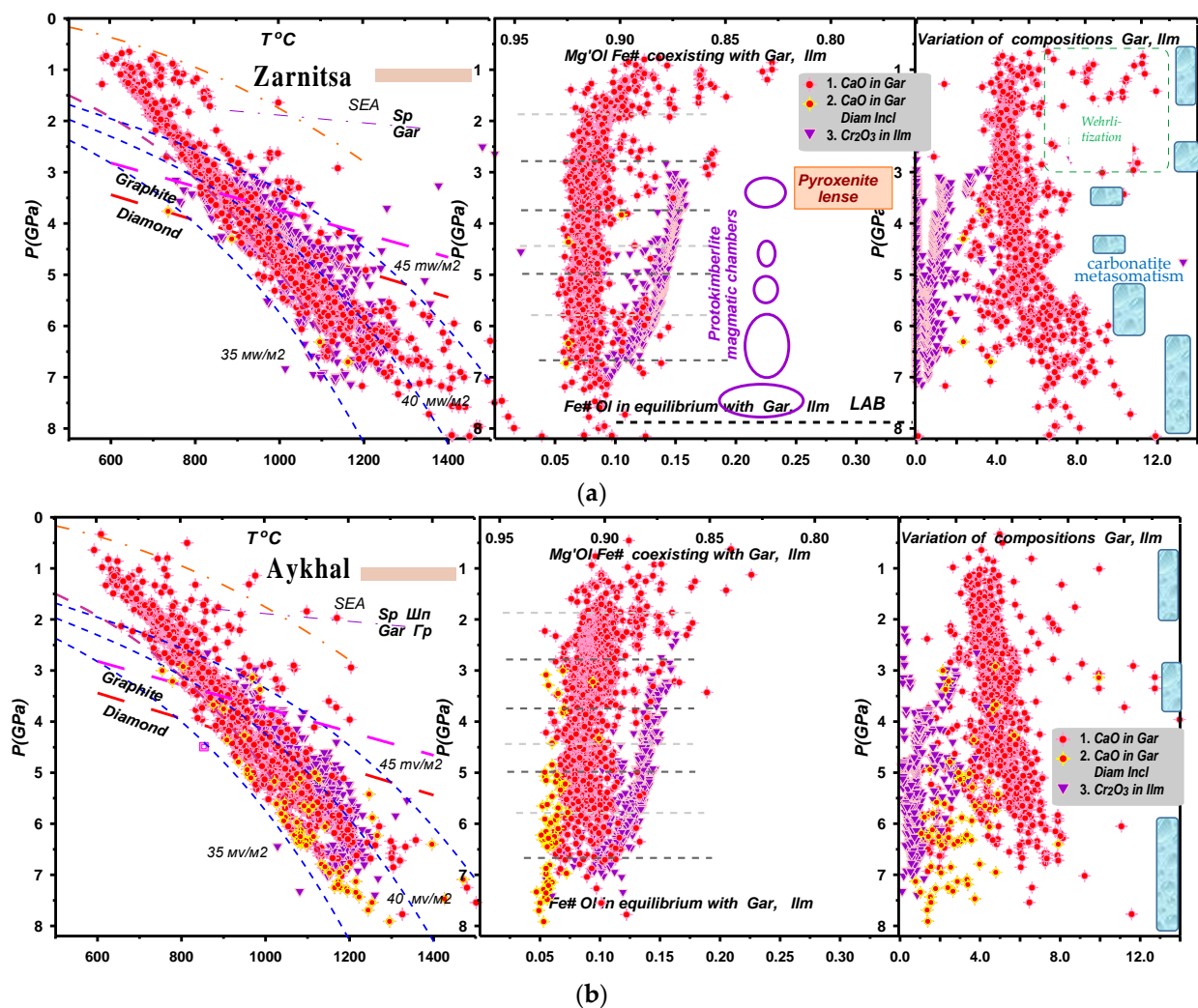


Figure 16. Cont.

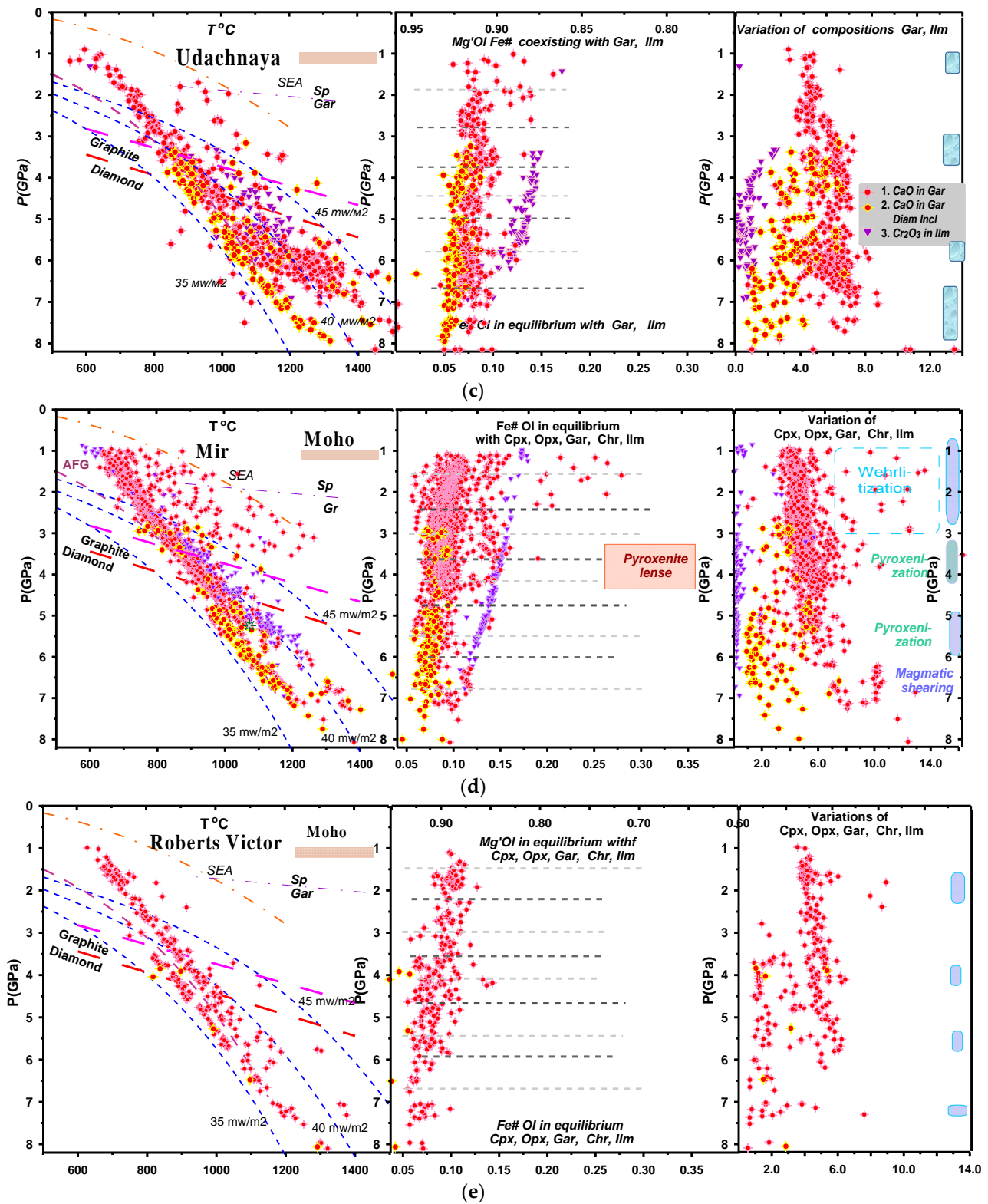


Figure 16. Reconstructions of the upper mantle sections beneath the Devonian kimberlite pipes in Central Yakutia, Daldyn, Alalkit, Malo-Botuobinsky fields, Siberia, and Roberts Victor, South Africa. Pressure and temperature estimates: for garnet: 1. T(°C) [97], P(GPa) [84]; 2. the same for diamond inclusions; for ilmenite—3. T(°C) [98], P(GPa) [85]. Zarnitsa (a), Aykhal (b). Udachnaya (c). Mir (d), Roberts Victor (e).

7. Conclusions

We showed that the classical model of dynamics of metasomatism for non-isothermal flow-type reservoir allows us to explain existing sudden spatial changes in xenolith composition of the mantle rocks and rock sequences beneath the in kimberlite pipes. It happens mainly along the trends of deep faults [2], It could explain the existence of various xenolith compositions in kimberlites and basalts of the Siberian craton. It also could to help to explain the the variations of the magmas in the southern folded areas framing SC [46,81,103]. It could regulate following phenomena.

- (1) The inflow of fluids of any composition from the upper-mantle magma chambers inevitably results in the formation of zonal metasomatic columns in the ultrabasic lithospheric mantle (within the permeable zones of deep faults)
- (2) The supply of petrogenic components of a magma source results in the transformation of depleted ultrabasic rocks of the lithospheric mantle into substrates which can be regarded as deep analogs or crust rodingites.
- (3) The other fluid compositions result in deep calcinations and noticeable salination of metasomated substrate, or 'garnitization' of the original ultrabasic matrix.
- (4) The above mentioned areas, a basification zone appears; this zone is changed by the zones of wehrlitization, amphibolization, and biotitization.

The above-mentioned physicochemical trends for the lithospheric mantle change provide us insights into the specific features of spatial and time relationships for subsequent stages of metasomatic processes developed under cratons [80]. It is possible to develop research in two aspects: (1) to construct hydrodynamic models that are more suitable for tectonic dynamics of deep faults (as permeable lithosphere zones) for various stages of their evolution, and (2) to create a more complete scheme that combines both hydrodynamics and physicochemical dynamics, when compared to existing model, in the approximation of parallel numerical analysis.

The reactions with proto-kimberlite the essentially carbonatitic melts may essentially decrease the diamond grade of these kimberlites due to carbon oxidation. However, this refers only to the latest carbonation in oxidized proto-kimberlite melts.

Supplementary Materials: The following supporting information can be downloaded at <https://www.mdpi.com/article/10.3390/min13030423/s1>. In the Supplementary File S1, Table S1: Statistical values for clusters and general statistics for rock groups of the Udachnaya–Vostochnaya pipe (Yakutsk); Table S2: Statistical values for clusters and general statistics for rock groups; Table S3: Contents of gases in the xenolith samples before and after heating in the flow reactor, and kinetics of gas release under incremental heating; Table S4: Compositions of vitreous segregations inside the sample and on its surface for sample UV-34, undulose lherzolite; Table S5: Physical and physicochemical parameters; Table S6: Composition of mineral association in zone III versus fluid composition at the system entry; Table S7: Composition of minerals of metasomatic association in zone I versus composition of independent components in R_0 ; Table S8: Compositions of pyroxene and garnet versus compositions of independent components in reactor R_0 ; Table S9: Physicochemical conditions for the manifestation of rodingite association without clinopyroxene in zone I. In the Table S10, the compositions of the volatiles and gaseous phases determined in the minerals from the mantle xenoliths File 1 contains the results of the numerical experiments using the program complex Selector-C.

Author Contributions: Conceptualization, V.S.; methodology, V.S., Y.P., A.T., K.C., I.A. and K.S.; software, K.C. and K.S.; investigation, Y.P., V.S., A.T. and K.S.; writing—original draft preparation, V.S. and Y.P.; writing—review and editing, A.T., K.C., I.A. and K.S. All authors have read and agreed to the published version of the manuscript.

Funding: This work was conducted as a state assignment of IGM SB RAS and received partial financial support as the RFBR grant 19-05-00788. This work was also supported by the Ministry of Science and Higher Education of the Russian Federation, Government tasks for the Institute of Geochemistry SB RAS and the Institute of Geology and Mineralogy SB RAS; and the governmental assignment in terms of the Project IX.129.1.4.

Data Availability Statement: Not applicable.

Acknowledgments: The authors thank V.V. Ryabov for the critical problem discussions.

Conflicts of Interest: The authors declare no conflict of interest.

References

1. Griffin, W.L.; Ryan, C.G.; Kaminsky, F.V.; O'Reilly, S.Y.; Natapov, L.M.; Win, T.T.; Kinny, P.D.; Ilupin, I.P. The Siberian lithosphere traverse: Mantle terranes and the assembly of the Siberian Craton. *Tectonophysics* **1999**, *310*, 1–35. [[CrossRef](#)]
2. Ashchepkov, I.V.; Vladyskin, N.V.; Ntaflos, T.; Downes, H.; Mitchel, R.; Smelov, A.P.; Rotman, A.Y.; Stegnitsky, Y.; Smarov, G.P.; Makovchuk, I.V.; et al. Regularities of the mantle lithosphere structure and formation beneath Siberian craton in comparison with other cratons. *Gondwana Res.* **2013**, *23*, 4–24. [[CrossRef](#)]
3. Avchenko, O.V.; Chudnenko, K.V.; Aleksandrov, I.L.; Khudolozhskaya, V.O.; Sharov, O.I. Solution of petrologic problems for metamorphic rocks using Program Complex SELECTOR. *Vestn. ONZ* **2010**, *2*, Z11002.
4. Wyllie, P.J. Experimental petrology of upper mantle materials, processes and products. *J. Geodyn.* **1995**, *20*, 429–468. [[CrossRef](#)]
5. Green, D.H.; Fallon, T.J. Primary magmas at mid-ocean ridges, “hotsports”, other intraplate settings: Constraints on potential temperature. In *Plates, Plumes, and Paradigms*; Foulger, G.R., Natland, J.H., Presnall, D.C., Anderson, D.L., Eds.; Geological Society of America: Boulder, CO, USA, 2005; Volume 388, pp. 217–247.
6. Spera, F.I. Carbon Dioxide in Igneous Petrogenesis: II. Fluid Dynamics of Mantle Metasomatism. *Contrib. Miner. Petrol.* **1981**, *77*, 56–63. [[CrossRef](#)]
7. Tomilenko, A.A. Fluid Regime of Mineral Formation in the Continental Lithosphere at High and Moderate Pressures According to the Data from Fluid and Melt Inclusions Study in Minerals. Ph.D. Thesis, UIGGM SB RAS, Novosibirsk, Russia, 2006.
8. Sharapov, V.N.; Tomilenko, A.A.; Perepechko, Y.V.; Chudnenko, K.V.; Mazurov, M.P. The physicochemical dynamics of evolution of fluid above asthenosphere systems beneath the Siberian Platform. *Russ. Geol. Geophys.* **2010**, *51*, 1037–1058. [[CrossRef](#)]
9. Sharapov, V.N.; Chudnenko, K.V.; Mazurov, M.P.; Perepechko, Y.V. Metasomatic zoning of subcratonic lithosphere in Siberia: Physicochemical modeling. *Russ. Geol. Geophys.* **2009**, *50*, 1107–1118. [[CrossRef](#)]
10. Chudnenko, K.V.; Avchenko, O.V.; Aleksandrov, I.A. Estimation of formation conditions of mineral megasystems from thermodynamic modeling. *Dokl. Earth Sc.* **2007**, *416*, 1132–1136. [[CrossRef](#)]
11. Holloway, J.R. Igneous fluid. In *Thermodynamic Modeling of Geological Materials: Minerals, Fluids, and Melts. Reviews in Geology*; Mineralogical Society of America: Washington, DC, USA, 1987; Volume 17, pp. 211–233.
12. Letnikov, F.A.; Karpov, I.K.; Kiselev, A.I.; Shkandrin, B.O. *Fluid Regime of the Earth's Crust and Upper Mantle*; Nauka: Moscow, Russia, 1977; 216p.
13. Kadik, A.A.; Lukanin, O.A. *Degassing of the Upper Mantle During Melting*; Nauka: Moscow, Russia, 1986; 97p.
14. Kadik, A.A.; Sobolev, N.V.; Zharkova, E.V.; Pokhilenko, N.P. Redox conditions of formation of diamond-bearing peridotite xenoliths from the Udachnaya kimberlite pipe (Yakutia). *Geokhimiya* **1989**, *8*, 1120–1135.
15. Saxena, S.K. Oxidation state of mantle. *Geoch. Cosmochim. Acta* **1989**, *53*, 89–95. [[CrossRef](#)]
16. Saxena, S.K.; Fai, Y. Fluid mixtures in the C-H-O system at high pressure and temperature. *Geochim. Cosmochem. Acta* **1988**, *52*, 505–512. [[CrossRef](#)]
17. Taylor, W.R.; Green, D.H. The role of reduced C-O-H fluids in mantle fluids partial melting. In Proceedings of the IV Int. Kimberlites Conference, Sydney, Australia, 11–15 August 1988.
18. Fedorov, I.I.; Chepurov, A.I.; Osorgin, N.Y.; Sokol, A.G.; Petrushin, E.I. Modeling of component composition of graphite- and diamond-equilibrated C-H-O fluid at high temperatures and pressures. *Russ. Geol. Geophys.* **1992**, *33*, 72–79.
19. Pokhilenko, L.N.; Fedorov, I.I.; Pokhilenko, N.P.; Tomilenko, A.A. Fluid regime of formation of mantle rocks according to chromatographic analysis and thermodynamic calculations. *Russ. Geol. Geophys.* **1994**, *35*, 67–70.
20. Kadik, A.A.; Zharkova, E.V.; Efimova, E.S.; Sobolev, N.V. Redox conditions for the formation of diamond crystals: Electrochemical study. *Dokl. Akad. Nauk.* **1997**, *357*, 671–675.
21. Zubkov, V.S. On the problem of composition and forms of fluid occurrence in the C-H-N-O-S system under the P-T conditions of the upper mantle. *Geokhimiya* **2001**, *2*, 131–145.
22. Kadik, A.A. Reduced fluids of the mantle: Connection with chemical differentiation of the planetesimal substance. *Geokhimiya* **2003**, *9*, 928–940.
23. Simakov, S.K. *Physicochemical Conditions of Formation of Diamond-Bearing Parageneses of Eclogites in the Rocks of Upper Mantle and the Earth's Crust*; SVNTs DVO RAN: Magadan, Russia, 2003; 157p.
24. Zubkov, V.S. *Thermodynamic Modeling of the System C-H-N-O-S under P-T Conditions of the Upper Mantle*; Vestnik GeoIGU: Irkutsk, Russia, 2005; 165p.
25. Bychinskii, V.A.; Karpov, I.K.; Koptev, A.V.; Chudnenko, K.V. Complete and metastable equilibrium of hydrocarbons in the Earth crust and upper mantle. *Nation. Geol.* **2005**, *2*, 65–74.
26. Anderson, T.; O'Reilly, S.Y.; Hofmann, A.W. The trapped fluid phase in upper mantle xenoliths from Victoria, Australia: Implications for mantle metasomatism. *Contr. Miner. Petrol.* **1984**, *88*, 72–85. [[CrossRef](#)]
27. Rosenbaum, J.M.; Zindler, F.; Rubenstone, J.L. Mantle fluids: Evidence from fluid inclusions. *Geochim. Cosmochem. Acta* **1996**, *60*, 3229–3252. [[CrossRef](#)]

28. Tomilenko, A.A.; Kovyazin, S.V.; Pokhilenko, L.N.; Sobolev, N.V. Primary hydrocarbon inclusions in garnet of diamond-bearing eclogite from the Udachnaya kimberlite pipe, Yakutia. *Dokl. Earth Sci.* **2009**, *426*, 695–698. [[CrossRef](#)]
29. Kut'yev, F.S.; Sharapov, V.N. *Petrogenesis of Subvolcanic Rocks*; Nedra: Moscow, Russia, 1979; 179p.
30. Osorgin, N.Y. *Chromatographic Analysis of Gas Phase in Minerals (Technique, Equipment, and Methodology)*; UIGGM SB RAS: Novosibirsk, Russia, 1990; Volume 11, 19p.
31. Pokhilenko, N.P.; Sobolev, N.V.; Kuligin, S.S.; Shimizu, N. Peculiarities of Distribution of Pyroxenite Paragenesis Garnets in Yakutian Kimberlites and Some Aspects of the Evolution of the Siberian Craton Lithospheric Mantle. In Proceedings of the VIIth International Kimberlite Conference, Cape Town, South Africa, 11–17 April 1998.
32. Sharapov, V.N.; Cherepanov, A.N.; Popov, V.N.; Rakhmenkulova, I.F. Shield Volcanoes of Siberian Flood Basalts: Dynamics of Lava Sheets Formation. In *Horizons in Earth Science Research*; Nova Science Publishers Inc.: Hauppauge, NY, USA, 2011; Volume 4, pp. 61–94.
33. Chepurov, A.I.; Tomilenko, A.A.; Shebanin, A.P.; Sobolev, N.V. Fluid inclusions in natural diamonds from the Yakutian placer deposits. *Dokl. Akad. Nauk* **1994**, *336*, 662–665.
34. Tomilenko, A.A.; Ragozin, A.L.; Shatskii, V.S.; Shebanin, A.P. Variations in the fluid phase composition in the process of natural diamond crystallization. *Dokl. Earth. Sci.* **2001**, *379*, 571–574.
35. Zhimulev, E.I.; Sonin, V.M.; Chepurov, A.I.; Tomilenko, A.A. Chromatographic study of conditions of formation of diamond crystals of rhombic-dodecahedron habitus. *Geol. Ore Deposit.* **2009**, *51*, 272–275. [[CrossRef](#)]
36. Chupin, V.P.; Tomilenko, A.A.; Chupin, S.V. Origin of granulite complexes: Results of study of melt and fluid inclusions in zircons and rock-forming minerals. *Russ. Geol. Geophys.* **1993**, *34*, 116–131.
37. Tomilenko, A.A.; Kovyazin, S.V. Formation of coronal structures around olivine in anorthosites of the Korosten pluton, Ukrainian shield: Mineralogy, geochemistry, and fluid inclusions. *Petrologiya* **2008**, *16*, 92–109.
38. Karpov, I.K.; Chudnenko, K.B.; Bychinskii, V.A. *SELECTOR (Program for the Calculation of Chemical Equilibria by Minimization of Thermodynamic Potentials)*; IGC SB RAS: Irkutsk, Russia, 1994; 123p.
39. Bashkirov, A.N.; Novak, F.I.; Loktev, S.M.; Kamzolkin, V.V. On catalytical activity of some natural silicate minerals in the synthesis from carbon oxide and hydrogen. *Chem. Techn. Fuel* **1956**, *3*, 38–40.
40. Taran, Y.A.; Novak, F.I.; Antoshchuk, I.A.; Bashkirov, A.N. Catalytical properties of volcanic rocks in the synthesis of hydrocarbon from carbonic oxide and hydrogen. *Dokl. Akad. Nauk SSSR* **1981**, *257*, 1158–1161.
41. Sharapov, V.N.; Ione, K.G.; Mazurov, M.P.; Mysov, V.M.; Perepechko, Y.V. *Geocatalysis and Evolution of the Mantle–Crust Magmatic Fluid Systems*; Academic Publishing House “Geo”: Novosibirsk, Russia, 2007; 186p.
42. Sharapov, V.N.; Kudryavtseva, O.P. Estimation of thermodynamic parameters of the Moho discontinuity beneath the area of trap development on the Siberian Platform and West Siberian Plate. *Russ. Geol. Geophys.* **2003**, *44*, 993–1005.
43. Tomilenko, A.A.; Shatsky, V.S.; Kovyazin, S.V.; Ovchinnikov, Y.I. Melt and fluid inclusions in anorthosite xenolith from of the Udachnaya kimberlites pipe, Yakutia. *Dokl. Earth Sci.* **2002**, *387*, 1060–1062.
44. Nikulin, V.I.; Lelyukh, M.I.; Fon-der-Flaas, G.S. *Diamond Prognosis*; ALROSA: Irkutsk, Russia, 2001; 211p.
45. Rotman, A.Y. Subalkaline Basic Rocks of Kimberlite-Governing Structures of the Eastern Part of Siberian Platform. Ph.D. Thesis, UIGGM SB RAS, Novosibirsk, Russia, 2002.
46. Kepezhinskas, V.V. *Cenozoic Alkali Basalts of Mongolia and Their Mantle Inclusions*; Nauka: Moscow, Russia, 1979; 305p.
47. Korzhinskii, D.S. *The Theory of Metasomatic Zoning*; Nauka: Moscow, Russia, 1969; 114p.
48. Golubev, V.S. *Dynamics of Geochemical Processes*; Nedra: Moscow, Russia, 1981; 206p.
49. Polyakov, G.V. (Ed.) *Model Analysis of Mantle–Crust Ore-Forming Systems*; Izd. SO RAN: Novosibirsk, Russia, 2009; 256p.
50. Chudnenko, K.V. *Thermodynamic Modeling in Geochemistry: Theory, Algorithms, Software, Applications*; Academic Publishing House “Geo”: Novosibirsk, Russia, 2010; 287p.
51. Khalatnikov, I.M. *Theory an Introduction to the Theory of Superfluidity*; CRC Press: Boca Raton, FL, USA, 1965; 224p.
52. Dorovsky, V.N. Mathematical models of two-velocity media. Part I. *Math. Comput. Model.* **1995**, *21*, 17–28. [[CrossRef](#)]
53. Dorovsky, V.N.; Perepechko, Y.V. Mathematical models of two-velocity media. Part II. *Math. Comput. Model.* **1996**, *24*, 69–80. [[CrossRef](#)]
54. Patankar, S. *Numerical Heat Transfer and Fluid Flow*; Hemisphere Publishing Corporation: New York, NY, USA, 1980; 151p.
55. Perepechko, L.N. Investigation of heat mass transfer processes in the boundary layer with injection. *Arch. Thermodyn.* **2000**, *21*, 41–54.
56. Perepechko, Y.V.; Sorokin, K.E. Two-velocity dynamics of compositional heterophase media. *J. Eng. Thermophys.* **2013**, *22*, 14–18. [[CrossRef](#)]
57. Perepechko, Y.V.; Sharapov, V.N. Dynamics of melting in the oceanic upper mantle. *Russ. Geol. Geophys.* **2001**, *42*, 1237–1248.
58. Sharapov, V.N.; Perepechko, Y.V.; Mazurov, M.P. Mantle-crustal fluid-magmatic systems of spreading zones. *Russ. Geol. Geophys.* **2006**, *47*, 1326–1343.
59. Sharapov, V.N.; Perepechko, Y.V.; Perepechko, L.N.; Rakhmenkulova, I.F. Mantle sources of Permian–Triassic traps (West Siberian plate and Siberian craton). *Russ. Geol. Geophys.* **2008**, *49*, 492–502. [[CrossRef](#)]
60. Vargaftik, N.B. *Manual on Thermophysical Properties of Gases and Liquids*; Gos. Izd. FML: Moscow, Russia, 1963; 698p.
61. Spiegelman, M.; Kelemen, P.; Aharonov, E. Causes and consequences of flow organization during melt transport: The reaction infiltration instability in compatible media. *J. Geophys. Res. Solid Earth* **2001**, *106*, 2061–2077. [[CrossRef](#)]

62. Sobolev, V.S.; Dobretsov, N.L.; Sobolev, N.V. (Eds.) *Deep-Seated Xenoliths and Upper Mantle*; Nauka: Novosibirsk, Russia, 1975; 255p.
63. Elliott, T.; Spiegelman, M. Melt migration in oceanic crustal production: A U-series perspective. In *The Crust. Treatise on Geochemistry*; Holland, H.D., Turekian, K., Eds.; Elsevier: Pergamon, Turkey, 2003; Volume 3, pp. 465–510.
64. Katz, R.; Weatherley, S. Consequences of mantle heterogeneity for melt extraction at mid-ocean ridges. *Earth Planet. Sci. Lett.* **2012**, *335–336*, 226–237. [[CrossRef](#)]
65. Shirey, S.B.; Cartigny, P.; Frost, D.Y.; Keshav, S.; Nestola, F.; Nimits, P.; Sobolev, N.V.; Walter, M.S. Diamonds and the geology of mantle carbon. *Rew. Mineral.* **2013**, *75*, 355–421. [[CrossRef](#)]
66. Sobolev, N.V. *The Deep-Seated Inclusions in Kimberlites and Problem of the Upper Mantle Composition*; Nauka: Novosibirsk, Russia, 1974; 247p.
67. Efimova, E.S.; Sobolev, N.V.; Pospelova, L.N. Sulfide inclusions in diamonds and specific features of paragenesis. *Zap. VMO* **1983**, *112*, 300–310.
68. Sobolev, N.V.; Efimova, E.S.; Koptil', V.I.; Lavrentiev, Y.G.; Sobolev, V.S. Inclusions of coesite, garnet, and omphacite in the Yakutian diamonds—The first finding of coesite paragenesis. *Dokl. Akad. Nauk SSSR* **1976**, *230*, 1441–1444.
69. Sobolev, N.V.; Efimova, E.S.; Pospelova, L.N. Native iron in diamonds of Yakutia and its paragenesis. *Russ. Geol. Geophys.* **1981**, *22*, 25–29.
70. Sobolev, N.V.; Logvinova, A.M.; Efimova, E.S. Syngenetic phlogopite inclusions in kimberlite-hosted diamonds: Implications for the role of volatiles in diamond formation. *Russ. Geol. Geophys.* **2009**, *50*, 1234–1248. [[CrossRef](#)]
71. Sobolev, N.V.; Logvinova, A.M.; Zedgenizov, D.A.; Pokhilenko, N.P.; Malygina, E.V.; Kuzmin, D.V.; Sobolev, A.V. Petrogenetic significance of minor elements in olivines from diamonds and peridotite xenoliths from kiberlites of Yakutia. *Lithos* **2009**, *1125*, 701–713.
72. White, W.M. *Geochemistry*; Elsevier: Amsterdam, The Netherlands, 1997; 700p.
73. De, A. Petrology of dikes emplaced in the ultramafic rocks of southeastern Quebec and origin of the rodingite. In *GSA Memoirs*; GeoScienceWorld: McLean, VA, USA, 1972; Volume 132, pp. 489–502.
74. Goles, G.G. Geochemistry of high-grade eclogites and metarodingites from the Central Alps. *Contrib. Mineral. Petrol.* **1981**, *76*, 301–311.
75. Esteban, J.J.; Cuevas, J.; Tubía, J.M.; Yusta, I. Xenotlite in rodingite assemblages from the Ronda peridotites, Betic Cordilleras Southern Spain. *Can. Mineral.* **2003**, *41*, 161–170. [[CrossRef](#)]
76. Pomonis, P.; Tsikouras, B.; Karipi, S.; Hatzipanagiotou, K. Rodingite formation in ultramafic rocks from the Koziaks ophiolite, Western Thessaly, Greece: Conditions of metasomatic alteration / geochemical exchanges T–X (CO₂) evolutionary path. *Can. Mineral.* **2008**, *46*, 569–581. [[CrossRef](#)]
77. Python, M.M.; Shibata, T.; Arai, S.; Python, M.; Yoshikawa, M.; Shibata, T.; Arai, S. Diopsidites and Rodingites: Serpentinisation and Ca-Metasomatism in the Oman Ophiolite Mantle. In *Dyke Swarms: Keys for Geodynamic Interpretation*; Springer: Berlin/Heidelberg, Germany, 2011; pp. 401–435.
78. Arai, S.; Ishimaru, S.; Okrugin, V.M. Metasomatized harzburgite xenoliths from Avacha volcano as fragments of mantle wedge of the Kamchatka arc: Implication for the metasomatic agent. *Island Arc* **2003**, *12*, 233–246. [[CrossRef](#)]
79. Srivastava, R. *Dyke Swarms: Keys for Geodynamic Interpretation*; Springer: Berlin/Heidelberg, Germany, 2011; pp. 401–435.
80. Solov'eva, L.V.; Vladimirov, B.M.; Dneprovskaya, L.V.; Maslovskaya, M.I.; Brandt, S.B. *Kimberlites and Kimberlite-Like Rocks. The Upper Mantle Substance under the Paleoplatforms*; Nauka: Novosibirsk, Russia, 1994; 250p.
81. Litasov, K.; Taniguchi, H. *Mantle Evolution Beneath the Baikal Rift*; Center for Northeast Asian Studies Tohoku University: Sendai, Japan, 2002; Volume 5, 221p.
82. Ryabov, V.V.; Shevko, A.Y.; Zateeva, S.N. 'Anomalous structures' in traps of Siberian Platform as index of geodynamic conditions for formation of platobasalts. *Lithosphere* **2005**, *4*, 165–177.
83. Kogarko, L.N. Role of deep fluids in genesis of mantle heterogeneities and alkali magmatism. *Russ. Geol. Geophys.* **2005**, *46*, 1234–1245.
84. Ashchepkov, I.V.; Ntaflos, T.; Logvinova, A.M.; Spetsius, Z.V.; Downes, H.; Vladykin, N.V. Monomineral universal clinopyroxene and garnet barometers for peridotitic, eclogitic and basaltic systems. *Geosci. Front.* **2017**, *8*, 775–795. [[CrossRef](#)]
85. Taylor, W.R.; Kammerman, M.; Hamilton, R. New thermometer and oxygen fugacity sensor calibrations for ilmenite and chromium spinel-bearing peridotitic assemblages. In *7th International Kimberlite Conference. Extended Abstracts*; Red Roof Design: Cape Town, South Africa, 1998; pp. 891–901.
86. Ashchepkov, I.V.; Logvinova, A.M.; Ntaflos, T.; Vladykin, N.V.; Downes, H. Alakit and Daldyn kimberlite fields, Siberia, Russia: Two types of mantle sub-terrane beneath central Yakutia? *Geosci. Front.* **2017**, *8*, 671–692. [[CrossRef](#)]
87. Golovin, A.V.; Sharygin, I.S.; Kamenetsky, V.S.; Korsakov, A.V.; Yaxley, G.M. Alkali-carbonate melts from the base of cratonic lithospheric mantle: Links to kimberlites. *Chem. Geol.* **2018**, *483*, 261–274. [[CrossRef](#)]
88. Kamenetsky, V.S.; Yaxley, G.M. Carbonate–silicate liquid immiscibility in the mantle propels kimberlite magma ascent. *Geochim. Et Cosmochim. Acta* **2015**, *58*, 48–56. [[CrossRef](#)]
89. Ashchepkov, I.V.; Alymova, N.V.; Logvinova, A.M.; Vladykin, N.V.; Kuligin, S.S.; Mityukhin, S.I.; Downes, H.; Stegnitsky, Y.B.; Prokopiev, S.A.; Salikhov, R.F.; et al. Picroilmenites in Yakutian kimberlites: Variations and genetic models. *Solid Earth* **2014**, *5*, 915–938. Available online: www.solid-earth.net/5/915/2014/ (accessed on 1 March 2022). [[CrossRef](#)]

90. Ashchepkov, I.; Medvedev, N.; Ivanov, A.; Vladykin, N.; Ntaflos, T.; Downes, H.; Saprykin, A.; Tolstov, A.; Vavilov, M.; Shmarov, G. Deep mantle roots of the Zarnitsa kimberlite pipe, Siberian craton, Russia: Evidence for multistage polybaric interaction with mantle melts. *J. Asian Earth Sci.* **2021**, *213*, 104756. [[CrossRef](#)]
91. Gervasoni, F.; Jalowitzki, T.; Rocha, M.P.; Kalikowski Weska, F.; Novais-Rodrigues, E.; de Freitas Rodrigues, R.A.; Bussweiler, Y.; Barbosa, E.S.R.; JBerndt, J.; Dantas, E.L.; et al. Recycling process and proto-kimberlite melt metasomatism in the lithosphere-asthenosphere boundary beneath the Amazonian Craton recorded by garnet xenocrysts and mantle xenoliths from the Carolina kimberlite. *Geosci. Front.* **2022**, *13*, 101429. [[CrossRef](#)]
92. Ionov, D.A.; Doucet, L.S.; Xu, Y.; Golovin, A.V.; Oleinikov, O.B. Reworking of Archean mantle in the NE Siberian craton by carbonatite and silicate melt metasomatism: Evidence from a carbonate-bearing, dunite-to-websterite xenolith suite from the Obnazhennaya kimberlite. *Geochim. Et Cosmochim. Acta* **2018**, *224*, 132–153. [[CrossRef](#)]
93. Pokhilenko, N.P.; Agashev, A.M.; Litasov, K.D.; Pokhilenko, L.N. Carbonatite metasomatism of peridotite lithospheric mantle: Implications for diamond formation and carbonatite-kimberlite magmatism. *Russ. Geol. Geophys.* **2015**, *56*, 280–295. [[CrossRef](#)]
94. Giuliani, A.; Kamenetsky, V.S.; Kendrick, M.A.; Phillips, D.; Wyatt, B.A.; Maas, R. Oxide, sulphide and carbonate minerals in a mantle polymict breccia: Metasomatism by proto-kimberlite magmas, and relationship to the kimberlite megacrystic suite. *Chem. Geol.* **2013**, *353*, 4–18. [[CrossRef](#)]
95. Kopylova, M.G.; Ma, F.; Tso, E. Constraining carbonation freezing and petrography of the carbonated cratonic mantle with natural samples. *Lithos* **2021**, *388–389*, 106045. [[CrossRef](#)]
96. Pernet-Fisher, J.F.; Barry P., H.; Day, J.M.D.; Pearson, D.; Woodland, S.; Agashev, A.M.; Pokhilenko, L.N.; Pokhilenko, N.P. Heterogeneous kimberlite metasomatism revealed from a combined He-Os isotope study of Siberian megacrystalline dunite xenoliths. *Geochim. Et Cosmochim. Acta* **2019**, *266*, 220–236. [[CrossRef](#)]
97. O'Neill, H.S.C.; Wood, B.J. An experimental study of Fe-Mg- partitioning between garnet and olivine and its calibration as a geothermometer. *Contrib. Mineral. Petrol.* **1979**, *70*, 59–70. [[CrossRef](#)]
98. Ashchepkov, I.V.; Pokhilenko, N.P.; Vladykin, N.V.; Logvinova, A.M.; Kostrovitsky, S.I.; Afanasiev, V.P.; Pokhilenko, L.N.; Kuligin, S.S.; Malygina, L.V.; Alymova, N.V.; et al. Structure and evolution of the lithospheric mantle beneath Siberian craton, thermobarometric study. *Tectonophysics* **2010**, *485*, 17–41. [[CrossRef](#)]
99. Ragozin, A.; Zedgenizov, D.; Kuper, K.; Palyanov, Y. Specific internal structure of diamonds from Zarnitsa kimberlite pipe. *Crystals* **2017**, *7*, 133. [[CrossRef](#)]
100. Ionov, D.A.; Qi, Y.-H.; Kang, J.T.; Golovin, A.V.; Oleinikov, O.B.; Zheng, W.; Anbar, A.D.; Zhang, Z.F.; Huang, F. Calcium isotopic signatures of carbonatite and silicate metasomatism, melt percolation and crustal recycling in the lithospheric mantle. *Geochimica Et Cosmochimica Acta* **2019**, *248*, 1–13. [[CrossRef](#)]
101. Bulanova, G.P.; Wiggers de Vries, D.F.; Pearson, D.G.; Beard, A.; Mikhail, S.; Smelov, A.P.; Davies, G.R. An eclogitic diamond from Mir pipe (Yakutia), recording two growth events from different isotopic sources. *Chem. Geol.* **2014**, *381*, 40–54. [[CrossRef](#)]
102. Sobolev, N.V.; Shatsky, V.S.; Zedgenizov, D.A.; Ragozin, A.L.; Reutsky, V.N. Polycrystalline diamond aggregates from the Mir kimberlite pipe, Yakutia: Evidence for mantle metasomatism. *Lithos* **2016**, *265*, 257–266. [[CrossRef](#)]
103. Ashchepkov, I.V. *Deep-Seated Xenoliths of the Baikal Rift*; Nauka: Novosibirsk, Russia, 1991; 160p.

Disclaimer/Publisher's Note: The statements, opinions and data contained in all publications are solely those of the individual author(s) and contributor(s) and not of MDPI and/or the editor(s). MDPI and/or the editor(s) disclaim responsibility for any injury to people or property resulting from any ideas, methods, instructions or products referred to in the content.